

# JCTC

Journal of Chemical Theory and Computation

## A General Database for Main Group Thermochemistry, Kinetics, and Noncovalent Interactions – Assessment of Common and Reparameterized (*meta*-)GGA Density Functionals

Lars Goerigk<sup>†,‡</sup> and Stefan Grimme<sup>\*,†</sup>

*Theoretische Organische Chemie, Organisch-Chemisches Institut, Universität Münster, Corrensstrasse 40 and NRW Graduate School of Chemistry, Universität Münster, Wilhelm-Klemm-Strasse 10, D-48149 Münster, Germany*

Received September 15, 2009

**Abstract:** We present a quantum chemistry benchmark database for general main group thermochemistry, kinetics, and noncovalent interactions (GMTKN24). It is an unprecedented compilation of 24 different, chemically relevant subsets that either are taken from already existing databases or are presented here for the first time. The complete set involves a total of 1.049 atomic and molecular single point calculations and comprises 731 data points (relative chemical energies) based on accurate theoretical or experimental reference values. The usefulness of the GMTKN24 database is shown by applying common density functionals on the (*meta*-)generalized gradient approximation (GGA), hybrid-GGA, and double-hybrid-GGA levels to it, including an empirical London dispersion correction. Furthermore, we refitted the functional parameters of four (*meta*-)GGA functionals based on a fit set containing 143 systems, comprising seven chemically different problems. Validation against the GMTKN24 and the molecular structure (bond lengths) databases shows that the reparameterization does not change bond lengths much, whereas the description of energetic properties is more prone to the parameters' values. The empirical dispersion correction also often improves for conventional thermodynamic problems and makes a functional's performance more uniform over the entire database. The refitted functionals typically have a lower mean absolute deviation for the majority of subsets in the proposed GMTKN24 set. This, however, is also often accompanied at the expense of poor performance for a few other important subsets. Thus, creating a broadly applicable (and overall better) functional by just reparameterizing existing ones seems to be difficult. Nevertheless, this benchmark study reveals that a reoptimized (i.e., empirical) version of the TPSS-D functional (oTPSS-D) performs well for a variety of problems and may meet the standards of an improved functional. We propose validation against this new compilation of benchmark sets as a definitive way to evaluate a new quantum chemical method's true performance.

### 1. Introduction

The benefit of evaluating quantum chemical methods by benchmarking them against accurate experimental or theoretical energies was first realized by Pople and co-workers. Their work

culminated into the so-called G2/97 test set<sup>1</sup> and the enhanced versions G3/99<sup>2</sup> and G3/05.<sup>3</sup> However, these works mainly focused on atomization energies (or, equivalently, heats of formation). Electron and proton affinities and ionization potentials of small molecules played an additional minor role.

Truhlar and co-workers extended the idea of benchmarking by introducing databases covering a wide variety of different physicochemical properties, e.g., proton affinities, atomization energies, interaction energies of noncovalently bound

\* Corresponding author. Telephone: (+49)-251-8336512. E-mail: grimmes@uni-muenster.de.

<sup>†</sup> Organisch-Chemisches Institut.

<sup>‡</sup> Northrhine Westphalia Graduate School of Chemistry.

systems, barrier heights and reaction energies of diverse reactions, spectroscopic properties, transition-metal systems, and catalytic processes.<sup>4–12</sup> Truhlar and co-workers were also the first to carry out overall statistical analyses of combinations of different test sets to obtain one final number (e.g., an overall mean absolute deviation, MAD) for each tested method. Such an analysis makes an evaluation of any quantum chemical method and a comparison with other approaches more feasible. Important and popular benchmark sets introduced by other groups are, for example, the S22 set for noncovalent systems by Hobza and co-workers,<sup>13</sup> and the ISO34<sup>14</sup> set for isomerization energies of organic molecules, and the ‘mindless-benchmark’ set (MB08–165)<sup>15</sup> developed recently in our laboratory.

Having access to a plethora of different published benchmark sets, the question is which combination of these is the best to obtain a thorough insight into a given quantum chemical method’s performance. First of all, the requirements for such a ‘set-of-sets’ are that a large cross-section of chemically relevant properties should be covered and that the specific subsets should be of an adequate size. Particularly for the evaluation of density functional theory (DFT) approximations, such a set is expected to be useful. Nowadays, it is well-known that a given density functional (DF), that performs well for a certain property, is not necessarily adequate for computing completely different types of systems. Actual research continues to develop DFs that are equally well applicable to a variety of different properties. Therefore, the aforementioned ‘set-of-sets’ would be a useful tool for determining whether this aim is reached or not. Furthermore, it can be sometimes seen that benchmark studies are only carried out for systems that are similar to those of the empirical fit sets with which the new functionals were generated. We think that it is crucial to distinguish between a fit and a validation set and that the latter one should also cover systems that were not included in the first one.

In this work, we present such a ‘set-of-sets’ (database), which covers a variety of 24 subsets for general main group thermochemistry, kinetics, and noncovalent interactions (GMTKN24). It covers atomization, relative, and reaction energies, electron and proton affinities, ionization potentials, barrier heights between conformers, and noncovalent interactions (inter- and intramolecular). The majority of sets is taken from the literature.<sup>1,5,8–10,13–37</sup> We also present new benchmark subsets that are combinations of already published data. These are the sets for barrier heights of pericyclic reactions (BHPERI), reaction energies involving small closed-shell molecules (G2RC), intramolecular London dispersion interactions (IDISP) and for cases that are difficult to treat with DFT methods (DC9). Furthermore, completely new sets were developed for this work. These are SIE11, the first set focusing on self-interaction error-related problems, and NBRC, describing oligomerization and hydrogen fragmentation reactions of ammonia/borane systems.

The GMTKN24 database’s composition reflects many years of experience in benchmarking and applications of DFT methods to ‘real-life’ chemical problems. The range of properties covered by the GMTKN24 data set outperforms,

to the best of our knowledge, all other combinations of databases that have been previously proposed. Therefore, we think that GMTKN24 is highly representative for chemistry (excluding transition-metal chemistry). We propose that any quantum chemical method, that performs well for the entire database, can be really regarded as an accurate, robust, and useful method. GMTKN24 itself is also robust in a sense that adding or deleting one or two subsets does not qualitatively change the overall rating for the quantum chemical method under investigation.

This study focuses mainly on the evaluation of density functionals at the (*meta*-)generalized gradient approximation level (GGA). These functionals are still very important for the computation of the energetics and geometries of large systems. Particularly the physics community benefits from using GGAs for the calculation of solids and surfaces. Because they can be correct for slowly varying densities, these semilocal functionals are, in principle, better suited for solids than for molecules. Since Lee–Yang–Parr (LYP) correlation is not correct for a uniform gas, the ‘LYP-based’ functionals are less satisfactory than the Perdew–Burke–Ernzerhof based (‘PBE-based’) functionals for the equilibrium properties of metals.<sup>38</sup> With our new database, we are now able to investigate this difference also for molecules.

However, besides investigating (*meta*-)GGA functionals, the applicability of ‘higher rung’ functionals (i.e., B3LYP-D<sup>39–41</sup> and B2PLYP-D<sup>30,31</sup>) will also be tested in this study. We also want to note that functionals performing well for main group molecules need not perform well for solids. In particular, the best functional for main group chemistry, of those tested here, is B2PLYP, which diverges for solid metals.

Current DFs depend on a varying number of parameters, and there are two philosophies for determining these. The first one is the requirement of fulfilling physical boundary conditions (e.g., recovery of the uniform electron gas result for constant densities). Authors favoring this first approach argue that a DF should be as *ab initio* as possible and should be based on physical grounds. In 2005, Perdew et al. gave a ‘recipe’ for such an approach.<sup>42</sup> Examples are PBE<sup>43</sup> and its successor TPSS.<sup>44</sup> Contrary to that, the other main strategy of determining parameters is fitting them to accurate reference data. Such empirical DFs are, e.g., B3LYP,<sup>39,40</sup> HCTH,<sup>45</sup> the M05,<sup>46,47</sup> M06,<sup>11,48,49</sup> and M08<sup>50</sup> classes of functionals and the double-hybrid functionals B2PLYP<sup>30</sup> and mPW2PLYP.<sup>51</sup>

In the past, though, it was shown that, independent of the strategy with which the parameters are obtained, there is no clear right or wrong regarding the actual parameter values. Different values are more or less useful for the application to different chemical problems. Evidence for this are revised versions (with varying names) of the PBE,<sup>52–57</sup> TPSS,<sup>58,59</sup> BP86,<sup>60</sup> PW,<sup>61</sup> B3LYP,<sup>62</sup> B2PLYP,<sup>16,63</sup> and mPW2PLYP<sup>16</sup> functionals. In passing, it is noted that the improved performance of the revised functional versions could not always be confirmed by other researchers (for revPBE see, e.g., ref 64), which highlights the need for accurate and comprehensive benchmark sets, as outlined above.

Particularly for (*meta*)-GGA functionals, a variety of exchange and correlation functionals were proposed in the past, and with common quantum chemical codes, it is quite easy to arbitrarily combine these with each other. When doing this, though, the important question arises, whether the parameters of a certain exchange functional are optimal when combining them with a specific correlation functional. For example, one may ask, whether BLYP<sup>65,66</sup> would yield better results if the parameters were optimized according to this specific combination of Becke1988 exchange<sup>65</sup> with LYP correlation.<sup>66</sup> To the best of our knowledge, such an investigation has not been carried out yet.

Furthermore, our experience showed that, e.g., for thermodynamic properties, the TPSS *meta*-GGA functional yields similar results as the PBE functional. This happens, though, at a higher numerical complexity due to the inclusion of the kinetic energy density. Do physical boundary conditions lead to restrictions that inhibit improved performance of a certain DF, like TPSS? Would lifting these restrictions improve TPSS's performance compared to PBE? Finally, it is justified to ask how far one can go with an empirical fitting procedure for DFs, in general.

In this systematic study, we try to answer these questions. Based on a well balanced fit set, the parameters of the BLYP, mPWLYP, PBE and TPSS functionals are fully reoptimized. This reoptimization is carried out with an empirical dispersion correction (DFT-D)<sup>41</sup> to take into account long-range London dispersion effects and to partially withdraw a medium-range description of London dispersion by the semilocal functional parts. We think that this provides a better picture of a given functional's true performance.

The optimized functionals and their original versions will be benchmarked against the here presented GMTKN24 database. This allows a thorough evaluation of their performance for energetics. Furthermore, geometry optimizations of small first- and second-row and transition-metal compounds have been carried out, and the resulting bond lengths are compared to experimental data.

This manuscript is structured as follows: In the following section, Section 2, an overview of the GMTKN24 database is given. In Section 3, the computational details are explained. Section 4 describes the reparameterization procedure, including an overview of the fit set and a description of each functional. In Section 5, the results for the application to the GMTKN24 set and the optimized geometries are discussed.

## 2. The GMTKN24 Database

The herein presented database for general main group thermochemistry, kinetics, and noncovalent interactions covers a large variety of 24 different, chemically relevant subsets (GMTKN24). In Figure 1, an overview of these subsets is given. For each set, on average, the easiest and most difficult reactions (for GGA functionals) are shown. In Table 1, short descriptions for each part of the GMTKN24 database are given, including the number of entries, the specification of the reference values, and the relevant citations. Note that none of the reference data include zero point vibrational energies (ZPVEs) or thermal (enthalpic)

corrections. The type and source of reference data are given separately for each subset. By comparing different quantum chemistry programs with each other, we made sure that each entry is reliable and that the results are reproducible. Different codes with different technical setups, but for the same functional/basis set combination, typically produce differences for MADs of about 0.1 kcal mol<sup>-1</sup> or less. Molecules that led to problems with orbital initial guesses or electronic-state symmetries were left out. We suggest to use an extended Hueckel initial orbital guess for open-shell species. All entries are shown in the Supporting Information, Tables S1–S24, and are available for download from our Web site.<sup>67</sup> The optimized coordinates of all systems can also be obtained from there. In total, the GMTKN24 database comprises 1.049 single point calculations and 731 data points (relative energy values).

**2.1. The MB08–165 Subset.** The ‘mindless-benchmark’ set (MB08–165) was recently introduced by Korth and Grimme.<sup>15</sup> It contains 165 randomly created so-called ‘artificial molecules’ (AMs) with varying constituencies. For these molecules, decomposition energies into their hydrides (for the main group elements 1–4) and homonuclear diatomics (main group elements 5–7) were calculated. For these reactions, estimated CCSD(T)/CBS reference values were computed. The reference data is listed in Table S1 of the Supporting Information. See ref 15 for more details on the creation of the AMs and the reaction schemes. In contrast to other benchmark sets, MB08–165 is less biased toward certain chemical aspects, as it just contains artificial systems. Korth and Grimme assessed a variety of density functionals and could reproduce nicely the Jacob's Ladder scheme,<sup>42</sup> with higher-rung functionals yielding better results. We chose MB08–165 to be the first subset of our benchmark study, as it can be regarded as one of the most important of all 24 subsets. Compared to the other subsets, it contains a large number of reference values and involves rather high reaction energies: 180 single point calculations have to be carried out to compute all 165 decomposition energies; the average absolute energy of these reactions is 117.2 kcal mol<sup>-1</sup>.

**2.2. The W4–08 Subset.** The W4–08 database by Karton et al. contains atomization energies of 99 small molecules.<sup>16</sup> The systems are dominated by dynamical correlation (e.g., H<sub>2</sub>O and CH<sub>4</sub>), and a few also include nondynamical correlation effects (e.g., O<sub>3</sub>, C<sub>2</sub>, and BN). Out of these 99 molecules, 16 are such multireference cases. Therefore, an additional analysis of this database without these cases is carried out (see Table 1). This subset is denoted as W4–08woMR. All reference data are based on W4 or higher levels of theory (see ref 16). For the complete W4–08 subset, 111 single point calculations have to be carried out. The average absolute atomization energy is 237.5 kcal mol<sup>-1</sup> for the whole set and 261.5 kcal mol<sup>-1</sup> for W4–08woMR. The W4–08 database is listed in the Supporting Information, Table S2.

**2.3. The G21IP and G21EA Subsets.** The G21IP subset contains 36 adiabatic ionization potentials of atoms and small molecules that were taken from the G2-1 set by Curtiss et al.<sup>17</sup> Note that G2-1 also includes the SH<sub>2</sub> molecule in its singlet and triplet, and N<sub>2</sub><sup>+</sup> in its <sup>2</sup>Π<sub>u</sub> state, which are

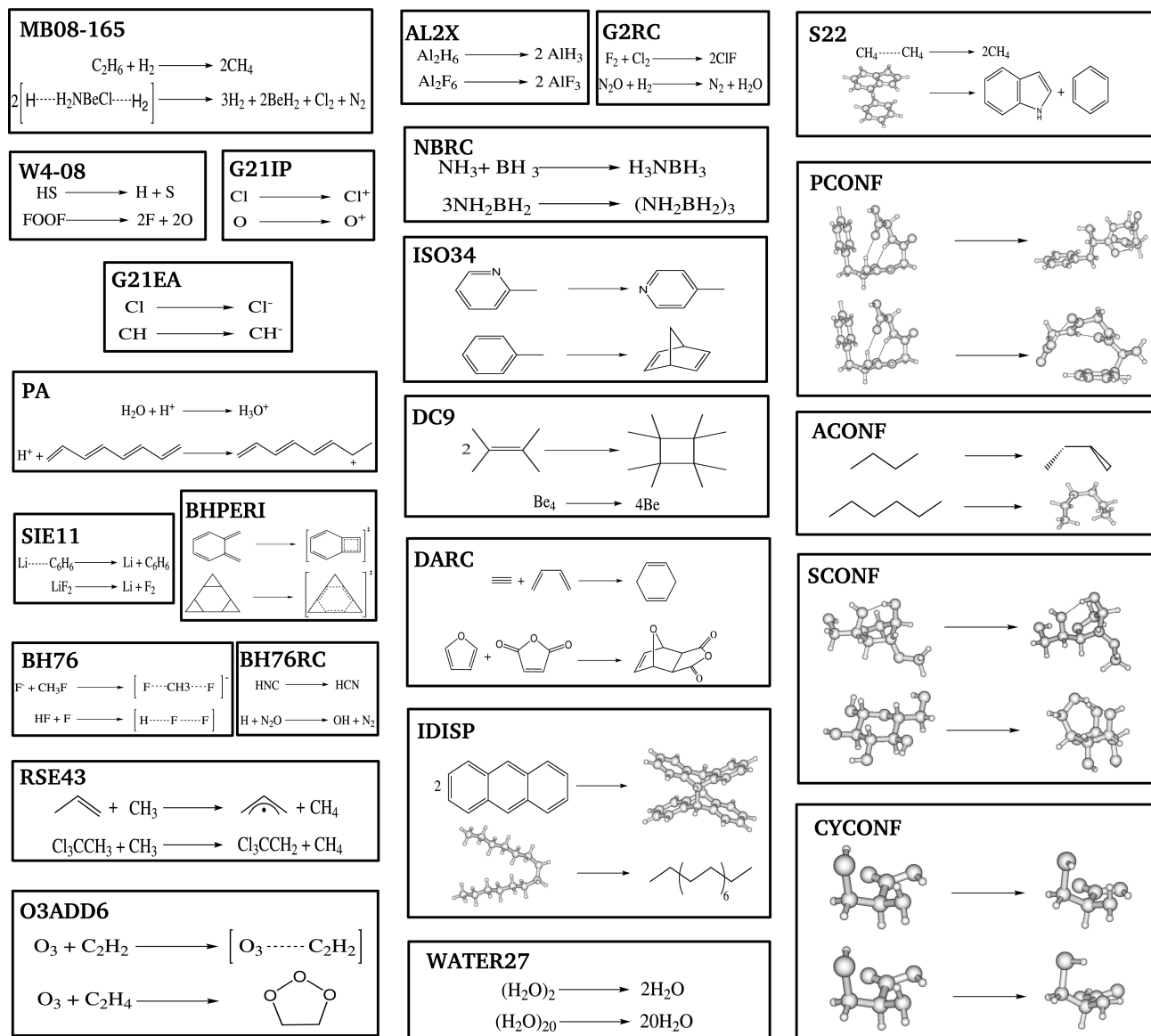


**Figure 1.** The subsets of the GMTKN24 database. For each set, on average, the easiest (top) and most difficult (bottom in each box) reactions (for GGAs) are shown.

problematic in unrestricted Kohn–Sham computations with some DFs. Thus, these cases were left out. The G21EA set contains 25 adiabatic electron affinities from the same work. Reference values are based on back-corrected experimental data. In total, 71 single point energies for G21IP and 50 for G21EA have to be calculated. The average absolute energies are 250.8 and 33.6 kcal mol<sup>-1</sup>, respectively. The G21IP and G21EA databases are listed in Tables S3 and S4 of the Supporting Information.

**2.4. The PA Subset.** The PA database includes 12 adiabatic proton affinities. On the one hand, the PA set includes eight small molecules (H<sub>2</sub>O, C<sub>2</sub>H<sub>2</sub>, SiH<sub>4</sub>, PH<sub>3</sub>, H<sub>2</sub>S, HCl, and H<sub>2</sub>) based on vibrationally back-corrected W1<sup>18,68</sup> reference values.<sup>18</sup> On the other hand, a homologous series of four conjugated polyenes (from ethene to all-*trans*-octatetraene) is included, that are taken from a study by Zhao and Truhlar.<sup>5</sup> Their reference values are based on estimated CCSD(T)/CBS results. Note that the polyenes from butadiene to octatetraene have a large impact on the complete subset's MAD because the results are influenced by the delocalization

error of density functionals. Therefore, they could also be made part of the self-interaction error subset (SIE11). However, from a chemical point of view, it is still justified to include them in the PA subset, as protonation of larger organic compounds is also a relevant issue that needs to be considered. In order to assess this subset, 24 single point energies have to be carried out. The average absolute reference energy is 174.9 kcal mol<sup>-1</sup>. The PA database is shown in Table S5 of the Supporting Information.

**2.5. The SIE11 Subset.** The self-interaction error (SIE) is a severe flaw in common DFT methods, and finding appropriate correction schemes is still on the agenda of actual research.<sup>69–73</sup> Although several studies have been carried out on the SIE and, although it also plays a role in some of the subsets included in GMTKN24 (barrier heights, proton affinities), a set which exclusively deals with the SIE has, to the best of our knowledge, not been proposed yet.

The SIE11 subset comprises 11 systems, which are extremely prone to the SIE. Five of these are positively charged, and seven systems are neutral. Examples, are the



**Table 1.** Description of the Subsets within the GMTKN24 Database

set	description	no.	av $ \Delta E ^a$	ref method	reference
MB08-165	decomposition energies of artificial molecules	165	117.2	est. CCSD(T)/CBS	<i>b</i>
W4-08	atomization energies of small molecules	99	237.5	W4	<i>c</i>
W4-08woMR	W4-08 without multi reference cases	83	261.5	W4	<i>c</i>
G21IP	adiabatic ionization potentials	36	250.8	expt.	<i>d</i>
G21EA	adiabatic electron affinities	25	33.6	expt.	<i>d</i>
PA	adiabatic proton affinities	12	174.9	est. CCSD(T)/CBS and W1	<i>e,f</i>
SIE11	self-interaction error related problems	11	34.0	est. CCSD(T)/CBS	this work
BHPERI	barrier heights of pericyclic reactions	26	19.4	W1 and CBS-QB3	<i>c,g,h,i,j</i>
BH76	barrier heights of hydrogen and heavy-atom transfers, nucleophilic substitution, unimolecular and association reactions	76	18.5	W1 and theor. est.	<i>k,l</i>
BH76RC	reaction energies of the BH76 set	30	21.5	W1 and theor. est.	<i>k,l</i>
RSE43	radical stabilization energies	43	7.5	est. CCSD(T)/CBS	<i>m</i>
O3ADD6	reaction and association energies and barrier heights for addition of O <sub>3</sub> to C <sub>2</sub> H <sub>4</sub> and C <sub>2</sub> H <sub>2</sub>	6	22.7	est. CCSD(T)/CBS	<i>n</i>
G2RC	reaction energies of selected G2/97 systems	25	50.6	expt.	<i>o</i>
AL2X	dimerization energies of AlX <sub>3</sub> compounds	7	33.9	expt.	<i>p</i>
NBRC	oligomerizations and H <sub>2</sub> fragmentations of NH <sub>3</sub> /BH <sub>3</sub> systems	6	30.2	est. CCSD(T)/CBS	this work
ISO34	isomerization energies of organic molecules	34	14.3	expt.	<i>q</i>
DC9	nine difficult cases for DFT	9	35.7	theor. and expt.	<i>i,r,s,t,u,v,w</i> , this work
DARC	reaction energies of Diels–Alder reactions	14	32.2	est. CCSDT/CBS	<i>p</i>
IDISP	intramolecular dispersion interactions	6	14.1	theor. and expt.	<i>q,x,y</i>
WATER27	binding energies of water, H <sup>+</sup> (H <sub>2</sub> O) <sub>n</sub> and OH <sup>−</sup> (H <sub>2</sub> O) <sub>n</sub> clusters	27	82.0	est. CCSD(T)/CBS;MP2/CBS	<i>z</i>
S22	binding energies of noncovalently bound dimers	22	7.4	est. CCSD(T)/CBS	<i>aa</i>
PCONF	relative energies of phenylalanyl–glycyl–glycine tripeptide conformers	10	1.5	est. CCSD(T)/CBS	<i>bb</i>
ACONF	relative energies of alkane conformers	15	1.8	W1h-val	<i>cc</i>
SCONF	relative energies of sugar conformers	17	4.9	est. CCSD(T)/CBS	<i>dd,ee</i> , this work
CYCONF	relative energies of cysteine conformers	10	2.1	est. CCSD(T)/CBS	<i>ff</i>

<sup>a</sup> Averaged absolute energies in kcal mol<sup>−1</sup>, excluding ZPVEs. <sup>b</sup> Ref 15. <sup>c</sup> Ref 16. <sup>d</sup> Ref 17. <sup>e</sup> Ref 18. <sup>f</sup> Ref 5. <sup>g</sup> Ref 19. <sup>h</sup> Ref 20. <sup>i</sup> Ref 21. <sup>j</sup> Ref 22. <sup>k</sup> Ref 8. <sup>l</sup> Ref 9. <sup>m</sup> Ref 23. <sup>n</sup> Ref 10. <sup>o</sup> Ref 1. <sup>p</sup> Ref 24. <sup>q</sup> Ref 14. <sup>r</sup> Ref 25. <sup>s</sup> Ref 26. <sup>t</sup> Ref 27. <sup>u</sup> Ref 28. <sup>v</sup> Ref 29. <sup>w</sup> Ref 30. <sup>x</sup> Ref 31. <sup>y</sup> Ref 32. <sup>z</sup> Ref 33. <sup>aa</sup> Ref 13. <sup>bb</sup> Ref 34. <sup>cc</sup> Ref 35. <sup>dd</sup> Ref 36. <sup>ee</sup> G. Csonka, private communication. <sup>ff</sup> Ref 37.

dissociation of He<sub>2</sub><sup>+</sup> into He and He<sup>+</sup>, the decomposition of LiF<sub>2</sub> into Li and F<sub>2</sub>, or the binding energy of the lithium–benzene complex. The complete subset, including reference data, is shown in Table S6 of the Supporting Information.

Geometries were optimized with SCS-MP2<sup>74</sup>/TZVPP,<sup>75</sup> except for the LiF<sub>2</sub> decomposition (PBE<sup>43</sup>/TZVPP). The reference data were obtained as estimated CCSD(T)<sup>76</sup>/CBS values as by Jurečka and Hobza.<sup>77</sup>

$$E^{\text{CCSD(T)/CBS}} \approx E^{\text{MP2/CBS}} + (E_{\text{corr}}^{\text{MP2/small basis}} - E_{\text{corr}}^{\text{CCSD(T)/small basis}}) \quad (1)$$

According to the formalism by Halkier et al.,<sup>78</sup> an extrapolation to the complete basis set limit on the MP2 level (from cc-pVTZ to cc-pVQZ)<sup>79</sup> was carried out, and the difference between MP2 and CCSD(T) correlation energies on the cc-pVDZ<sup>79</sup> level was added (eq 1). For the LiF<sub>2</sub> decomposition, this difference was calculated with the cc-pVTZ basis.

The complete SIE11 subset involves 29 single point calculations and has an average absolute reaction energy of 34.0 kcal mol<sup>−1</sup>.

**2.6. The BHPERI Subset.** The BHPERI subset contains 26 barrier heights of pericyclic reactions. The systems are taken from three publications and are shown in Table S7 of the Supporting Information. Ten reactions are taken from a work by Guner et al.<sup>19</sup> They include, among others, the ring-opening reaction of cyclobutene, the intramolecular Diels–

Alder reaction of *cis*-1,3,5-hexatriene, and the intermolecular Diels–Alder reaction of *cis*-butadiene with ethene. Reference values were based on CBS-QB3 calculations. Recently, Karton et al. published W1 reference values for 8 of these 10 reactions.<sup>16</sup> For the present study, we chose these eight W1 and the remaining two CBS-QB3 values as reference data. Furthermore, BHPERI includes nine 1,3-dipolar cycloadditions that were taken from a publication by Ess and Houk,<sup>20</sup> with improved reference values by Grimme et al. (CBS-QB3).<sup>21</sup> These reactions are based on diazonium, azomethine, and nitrilium betaines as 1,3-dipolar species. Finally, seven Diels–Alder reactions of different dienes with ethene are taken from the work of Dinadayalane et al. (CBS-QB3 reference values).<sup>22</sup> The final BHPERI set involves 61 single point calculations and has an average barrier height of 19.4 kcal mol<sup>−1</sup>.

**2.7. The BH76 and BH76RC Subsets.** The BH76 subset is a combination of the HTBH38<sup>8</sup> and NHTBH38<sup>9</sup> databases by Truhlar and co-workers. HTBH38 contains forward and reverse barriers of 19 hydrogen atom transfer reactions. NHTBH38 comprises 38 barriers of 19 heavy-atom transfer, nucleophilic substitution, unimolecular, and association reactions. Reference values are based on W1 calculations and ‘best theoretical estimates’ (see refs 8 and 9 for more details). The combined BH76 test set involves 95 single point calculations and has an average barrier height of 18.5 kcal mol<sup>−1</sup>. It is shown in Table S8 of the Supporting Information.

Having calculated the necessary reactants and products of the above-mentioned 36 reactions, it is straightforward to also compute the corresponding reaction energies. These are combined to another subset, denoted by BH76RC. In 6 of the 36 reactions, the reactants and products are identical (e.g.,  $\text{H} + \text{FH} \rightarrow \text{HF} + \text{H}$ ), and therefore, the BH76RC set contains only 30 reactions. Reference values were calculated from reference data of the BH76 set. The final BH76RC set has an average reaction energy of  $21.5 \text{ kcal mol}^{-1}$  and is listed in Table S9 of the Supporting Information.

**2.8. The RSE43 Subset.** The RSE43 subset contains 43 radical stabilization energies (RSE), defined as H-abstraction energies for the reactions of hydrocarbons with a methyl radical (see ref 80 for a thorough discussion of RSEs). All relevant structures (B3LYP/TZVP) and reference values (est. CCSD(T)/CBS) are taken from a recent work by Neese et al.<sup>23</sup> Note that their study included the acetyl radical, which was herein excluded from the RSE43 set due to state ordering problems. The complete set comprises 88 single point calculations and has an average absolute RSE of  $7.5 \text{ kcal mol}^{-1}$  (Table S10, Supporting Information).

**2.9. The O3ADD6 Subset.** Recently, Zhao et al. carried out an assessment of a variety of different quantum chemical methods for the thermochemical properties of a multireference system.<sup>10</sup> They studied the addition reactions of ozone to ethane and ethyne. For each reaction the formation energy of the primary ozonide, the barrier height and the association energy of the van der Waals (vdW) complex were calculated. Geometries were based on M05/MG3S calculations, and reference values were obtained at the estimated CCSD(T)/CBS level. In this work, the same systems are investigated, and the resulting test set is denoted by O3ADD6. Geometries and reference data are the same as in the work by Zhao et al. The complete database includes nine single point calculations. The average absolute energy is  $22.7 \text{ kcal mol}^{-1}$ . The O3ADD6 subset is listed in Table S11 of the Supporting Information.

**2.10. The G2RC Subset.** The G2RC subset contains 25 reactions, whose reactants and products are part of the G2/97 set of heats of formation.<sup>1</sup> Based on vibrationally back-corrected experimental data from ref 1, reference energies were calculated. The 25 reactions and their reference values are shown in Table S12 of the Supporting Information. The G2RC set comprises 47 single point calculations and has an average absolute reaction energy of  $50.6 \text{ kcal mol}^{-1}$ . It contains similar (small) molecules as already included in BH76RC, which allows cross-checking, and is a test for internal consistency of the results for different methods.

**2.11. The AL2X Subset.** In 2008, Johnson et al. reported a systematic study of delocalization errors in density functionals and their implication for main group thermochemistry.<sup>24</sup> Their study contained, among others, a test set for the calculation of the binding energies of the dimers of seven aluminum compounds of the type  $\text{AlX}_3$  ( $\text{X} = \text{H}, \text{CH}_3, \text{F}, \text{Cl}, \text{and Br}$ ). As reference values, they used back-corrected experimental data. Here we denote this test set by AL2X. For this subset, 13 single point calculations have to be carried out. The average absolute dimerization energy is  $33.9 \text{ kcal}$

$\text{mol}^{-1}$ . The AL2X database is shown in Table S13 in the Supporting Information.

**2.12. The NBRC Subset.** The formation of nitrogen–boron bonds is sometimes difficult to describe with DFT methods, and indeed, the investigation of ammonia–borane adducts gave first evidence for problems of the popular B3LYP functional.<sup>81</sup> In this study, we present a new benchmark set, called NBRC, which describes oligomerization and hydrogen fragmentation reactions of ammonia/borane systems. It consists of six reactions, which are shown in Table S14 of the Supporting Information. These reactions are the dimerization of ammonia with borane to the  $\text{NH}_3\text{BH}_3$  adduct, the  $\text{H}_2$  abstraction yielding  $\text{NH}_2\text{BH}_2$ , and the subsequent dehydrogenation to NHBH. Furthermore, three cyclization reactions of  $\text{NH}_2\text{BH}_2$  to the four-membered  $(\text{NH}_2\text{BH}_2)_2$  and the six-membered borazine and  $(\text{NH}_2\text{BH}_2)_3$  rings are considered. The reference values are based on estimated CCSD(T)/CBS computations (eq 1). The MP2/CBS limit was obtained from an aug-cc-pVTZ/QZ<sup>82</sup> extrapolation. The difference between the CCSD(T) and MP2 correlation energies was obtained with the cc-pVTZ basis. Effects due to the frozen core approximation were estimated at the MP2/cc-pwCvTZ<sup>79</sup> level. Geometries are based on PBE0<sup>83</sup>/TZVP<sup>75</sup> calculations. In order to calculate all reaction energies of the NBRC set, nine single point calculations have to be carried out. The average absolute reaction energy is  $30.2 \text{ kcal mol}^{-1}$ .

**2.13. The ISO34 Subset.** In 2007, Grimme et al. carried out an evaluation of quantum chemical methods for the calculation of 34 organic isomerization reactions (ISO34,<sup>14</sup> originally from refs 84 and 85). It turned out that some of these reactions are challenging tasks for common density functionals and that a benchmark study of new methods should include these types of reactions. These authors listed back-corrected experimental reference data that are also used in our work (see ref 14). The ISO34 set includes 63 single point calculations and has an average isomerization energy of  $14.3 \text{ kcal mol}^{-1}$ . It is shown in Table S15 of the Supporting Information.

**2.14. The DC9 Subset.** The DC9 subset comprises nine reactions that were shown to be difficult to treat with DFT methods. An overview of the DC9 set is given in Table S16 of the Supporting Information. The first system was discussed by Piacenza and Grimme, who carried out a systematic quantum chemical study on DNA base tautomers.<sup>25</sup> Among others, they investigated the tautomeric 2-pyridone/2-hydroxypyridine system. The reference value was obtained from QCISD(T)/TZV(2df,2pd)//B3LYP/TZV(2df,2pd) calculations. Note that the absolute reference value is rather small compared to that of the other reactions of this set. For many DFs, it is particularly difficult to predict the correct sign for this reaction, and deviations are often of the same magnitude as the actual reference value. Thus, although this reaction plays only a minor role in the overall statistics (note that, therefore, the second easiest reaction is shown in Figure 1), we still regard it as being important and, consequently, made it part of the DC9 subset.

The second entry describes the relative energy between the  $\text{C}_{20}$  cage and its bowl isomer. The structures were taken from the work by Grimme and Mück-Lichtenfeld.<sup>86</sup> The

reference value was computed here at the estimated CCSD(T)/CBS level (eq 1; MP2/CBS, difference between CCSD(T)/cc-pVDZ and MP2/cc-pVDZ correlation energies).

The third case was taken from Woodcock et al.<sup>26</sup> They discussed the fact that DFT methods sometimes yield problematic results for the energetic differences between cumulenes and poly-ynes. Among others, they studied the energy separation of the hepta-1,2,3,5,6-hexaene and hepta-1,3,5-triyne ( $C_7H_4$ ) isomers. The reference value is based on CCSD(T)/cc-pVTZ//MP2/cc-pVTZ calculations.

The fourth case is the dimerization of tetramethyl-ethene to octamethyl-cyclobutane. The reference value was calculated here on the SCS-MP2/TZVPP level of theory.

In 2006, Schreiner et al. published a study on the relative energies of several  $(CH)_{12}$  isomers and showed that many DFs failed to correctly describe these energies.<sup>27</sup> For this work, two isomers were chosen that are labeled with the numbers 1 and 31 in the work of Schreiner et al. (see ref 27 for structures).

The sixth reaction is taken from a work by Lepetit et al., which dealt with an assessment of density functionals on carbo-[*n*]-oxocarbons and on their valence isomers.<sup>28</sup> For the DC9 set, carbo-[3]-oxacarbon and its valence isomer, as shown in ref 28, were taken from their work. Reference data, though, were recalculated here. They are based on an estimated QCISD(T)<sup>76</sup>/CBS level of theory (SCS-MP2/CBS with cc-pVTZ and cc-pVQZ; difference between the QCISD(T)/cc-pVDZ and SCS-MP2/cc-pVDZ correlation energies).

The seventh entry is the reaction energy for the 1,3-dipolar cycloaddition between ethene and diazomethane. This reaction was studied by Grimme et al.<sup>21</sup> and the reference value was determined at the CBS-QB3 level.

The eighth reaction describes the decomposition of a  $Be_4$  cluster into beryllium atoms. The structure and reference value (CCSD(T)/CBS) were taken from a study by Lee.<sup>29</sup>

The last entry is the reaction of diatomic  $S_2$  to the  $S_8$ . This reaction was also part of the first study of the double-hybrid functional B2PLYP.<sup>30</sup> The experimental reference value and the geometries were taken from that study (see ref 30 for more details).

The complete DC9 database includes 19 single point calculations. The average reaction energy is 35.7 kcal mol<sup>-1</sup>.

**2.15. The DARC Subset.** In their work on the delocalization errors of DFT methods, Johnson et al. also investigated 14 typical Diels–Alder reactions.<sup>24</sup> These are the reactions of butadiene, cyclopentadiene, cyclohexadiene, and furane with ethene, ethyne, maleine, and maleinimide acting as dienophiles. Reference values are based on CCSD(T)/CBS calculations. The complete DARC database comprises 22 single point calculations. The average reaction energy is 32.2 kcal mol<sup>-1</sup>. It is listed in Table S17 in the Supporting Information.

**2.16. The IDISP Subset.** The IDISP set covers intramolecular London dispersion effects of large organic systems. The complete set and its reference values are shown in Table S18 of the Supporting Information. The first and the last two systems are taken from a study by Schwabe and Grimme.<sup>31</sup> These are the dimerization of anthracene, the hydrogenation

reaction of [2.2]paracyclophane yielding *p*-xylene, and the energetic differences between the linear and folded conformers of the  $C_{14}H_{30}$  and  $C_{22}H_{46}$  hydrocarbons. Structures and reference values were taken from the study by Schwabe and Grimme. They are based on theoretical or experimental data (see ref 31 for more details). The third reaction, in Table S18, is the isomerization of *n*-octane to iso-octane, which is also part of the ISO34 database.<sup>14</sup> The fourth reaction is the isomerization of *n*-undecane to 2,2,3,3,4,4-hexamethylpentane, which was shown in 2006 to be a problematic case for DFT methods by Grimme.<sup>32</sup> The reference value for this reaction is based on the SCS-MP2/cQZV3P//MP2/TZVP level of theory. The complete IDISP set involves 13 single point calculations. The average relative energy is 14.1 kcal mol<sup>-1</sup>.

**2.17. The WATER27 Subset.** Recently, Vyacheslav et al. published a DFT study on the binding energies of water clusters.<sup>33</sup> Their assessment was based on 27 neutral  $(H_2O)_n$ , positively charged  $H^+(H_2O)_n$ , and negatively charged  $OH^-(H_2O)_n$  clusters. As structures, their optimized B3LYP/6-311++G(2d,2p) geometries were taken. Reference data are based on either CCSD(T)/CBS or MP2/CBS calculations. We included this benchmark set as it can be regarded as a tough test for the description of strong hydrogen bonds and of long-range interactions. In the following, this set is denoted by WATER27. In total, 30 single point calculations have to be carried out for this set. The average binding energy of these clusters is 82.0 kcal mol<sup>-1</sup>. The complete set is listed in Table S19 in the Supporting Information.

**2.18. The S22 Subset.** The S22 set was introduced in 2006 by Jurečka et al.<sup>13</sup> Since then it has become a very popular benchmark set for studying noncovalent interactions. It includes the binding energies of seven hydrogen bonded dimers, eight complexes with predominant London dispersion interactions, and seven mixed complexes, where both hydrogen bonds and dispersion effects are important. Geometries are based on CCSD(T) or MP2 calculations. Reference data are estimated CCSD(T)/CBS values (see ref 13 for more details). The complete set comprises 57 single point calculations. Its average binding energy is 7.4 kcal mol<sup>-1</sup>. The S22 set is listed in Table S20 in the Supporting Information.

**2.19. The PCONF Subset.** In 2005, Řeha et al. carried out a thorough conformational study for the phenylalanyl–glycyl–glycine tripeptide.<sup>34</sup> Herein, we present a database denoted by PCONF, which is part of Řeha and co-workers' so-called 'Set 3' (see ref 34 for more details). In fact, we took the structures of the eleven most stable conformers of that particular set, which were obtained at the RI-MP2/cc-pVDZ level of theory. The relative energies, with respect to the most stable conformer, were calculated by Řeha et al. at the estimated CCSD(T)/CBS level of theory. These 10 relative energies, which are used as reference data for our study, have an average value of only 1.5 kcal mol<sup>-1</sup>. The complete PCONF set is shown in Table S21 in the Supporting Information.

**2.20. The ACONF Subset.** The ACONF subset comprises 15 relative energies of *n*-butane, *n*-pentane and *n*-hexane conformers. The relative energies are based on the



completely staggered conformation for each molecule. Geometries and reference values are taken from a recent work by Gruzman et al.<sup>35</sup> The latter ones are based on W1h-val calculations. The complete set comprises 18 single point calculations and has an average absolute energy of only 1.8 kcal mol<sup>-1</sup> (Table S22, Supporting Information).

**2.21. The SCONF Subset.** Recently, Csonka et al. carried out an evaluation study of DFs and of basis sets for a variety of different carbohydrate conformers.<sup>36</sup> They presented 3 test sets consisting of 15 D-allopyranose conformers (ALL15), 15 conformers of the five-membered ring system 3,6-anhydro-4-O-methyl-D-galactitol (AnGol15), and 4  $\beta$ -D-glucopyranose conformers (GLC4). For each test set, Csonka et al. calculated the energetic differences relative to each most stable conformer.

The herein considered subset called SCONF combines the AnGol15 and GLC4 sets of Csonka et al. Geometries are based on their B3LYP/6-31+G\* calculations. As reference data, the authors used MP2/aug-cc-pVTZ(-f) values. We regard this level of theory as insufficient and recalculated the reference data. For the AnGol15 subset the reference values are based on an estimated CCSD(T) extrapolation (eq 1). The MP2/CBS limit is based on aug-cc-pVDZ and aug-cc-pVTZ calculations. The difference between CCSD(T) and MP2 correlation energies was estimated with the cc-pVDZ basis set. The reference values for the GLC4 set were provided by Csonka in a private communication (MP2/CBS with aug-cc-pVTZ and aug-cc-pVQZ; difference between CCSD(T)/cc-pVTZ and MP2/cc-pVTZ). The reference values are shown in Table S23 of the Supporting Information. The notation of the different conformers is the same as in the original work (see ref 36 for more details). Compared to the original MP2 reference data, one can clearly see a difference between those and the herein presented CCSD(T)/CBS data.

The complete SCONF subset comprises 19 single point calculations and has an average conformational energy of 4.9 kcal mol<sup>-1</sup>.

**2.22. The CYCONF Subset.** The CYCONF subset contains 10 relative energies of 11 cysteine conformers that were recently studied by Wilke et al.<sup>37</sup> Reference values are based on estimated CCSD(T)/CBS calculations (see ref 37 for more details). The average relative energy of this set is only 2.1 kcal mol<sup>-1</sup> (Table S24, Supporting Information).

### 3. Computational Details

The CCSD(T)<sup>76</sup> calculations for obtaining reference data were done with MOLPRO Version 2006.1.<sup>87</sup> For QCISD(T)<sup>76</sup> calculations, the program RICC developed in our group was used.<sup>88</sup> All other calculations were carried out with a modified version of TURBOMOLE 5.9.<sup>89–92</sup> In general, the large Ahlrichs' type quadruple- $\zeta$  basis sets def2-QZVP were applied<sup>93</sup> that yield results quite close to the Kohn–Sham limit. For the calculations of electron affinities, diffuse s- and p-functions (for hydrogen only an s-function) were added from the Dunning aug-cc-pVQZ basis sets;<sup>82</sup> the resulting set is denoted by aug-def2-QZVP. Preliminary calculations for the WATER27 database showed that the results are very

basis set dependent. As negatively charged species are included in this set, we decided to add one diffuse s- and one diffuse p-function (taken from aug-cc-pVQZ) for oxygen. For example, this procedure reduced the MAD for this set from 8.2 to 3.8 kcal mol<sup>-1</sup> in the case of BLYP-D.

For all (*meta*)-GGA calculations, the resolution of the identity (RI-J) approximation was applied.<sup>94</sup> For B3LYP<sup>39,40</sup> and the DFT part of B2PLYP,<sup>30</sup> the RI-JK approximation was applied.<sup>95</sup> For the perturbative part of the B2PLYP functional, the RI approximation was used as well.<sup>92</sup> Auxiliary basis functions were taken from the TURBOMOLE basis set library.<sup>96</sup> In all cases, SCF convergence criteria were set to 10<sup>-7</sup> E<sub>h</sub> and the TURBOMOLE grid m4 was used.<sup>94</sup> All open-shell calculations were done within the unrestricted Kohn–Sham formalism (UKS). Geometry optimizations with the (*meta*)-GGAs were carried out with a convergence criterion of 10<sup>-7</sup> E<sub>h</sub>, regarding the changes of the total energy between two subsequent optimization cycles.

The refitting procedure was applied to the BLYP,<sup>65,66</sup> mPWLYP,<sup>61,66</sup> PBE,<sup>43</sup> and TPSS<sup>44</sup> functionals. This procedure and subsequent benchmark calculations were carried out with the empirical dispersion correction, developed by Grimme (DFT-D).<sup>41</sup> This correction ( $E_{\text{disp}}$ ) is added to the conventional Kohn–Sham DFT self-consistent field total energy  $E_{\text{KS-DFT}}$  (eq 2):

$$E_{\text{DFT-D}} = E_{\text{KS-DFT}} + E_{\text{disp}} \quad (2)$$

with

$$E_{\text{disp}} = -s_6 \sum_{i=1}^{N-1} \sum_{j=i+1}^N \frac{C_6^{ij}}{R_{ij}^6} f_{\text{dmp}}(R_{ij}) \quad (3)$$

where  $E_{\text{disp}}$  is the dispersion energy,  $C_6^{ij}$  denotes the dispersion coefficient for atom pair  $ij$ ,  $s_6$  is a global scaling parameter, and  $R_{ij}$  is an interatomic distance. To avoid near singularities for small  $R$  and for electron correlation double-counting, a damping function  $f_{\text{dmp}}$  is applied, which is given by

$$f_{\text{dmp}}(R_{ij}) = \frac{1}{1 + e^{-d(R_{ij}/R_c - 1)}} \quad (4)$$

Here,  $d = 20$  is a damping parameter and  $R_c$  is the sum of atomic vdW radii. There is overwhelming empirical evidence that the actual value of  $d$  (e.g., in a reasonable range between  $d = 15$ – $25$ ) has only a minor impact on the results. For a more detailed description of the dispersion correction, see ref 41.

The DFT-D approach uses a scale factor to derive the atomic vdW radii ( $r_{\text{scal}}^{\text{vdW}} = 1.1$  in the original work) from computed atomic electron densities. These original radii, however, lead to small double-counting effects with some functionals. Preliminary investigations carried out for this work showed that this choice of the scale factor, in particular, influences the description of hydrogen bonds. Therefore, we decided to rescale the radii in Table 1 of ref 41 by 1.04545 (i.e.,  $r_{\text{scal}}^{\text{vdW}} = 1.15$ ) for all reoptimized functionals. Furthermore, a fixed  $s_6$  value of unity gives an asymptotically correct and consistent description of the London dispersion energy. Applying the DFT-D correction during the fitting procedure,



furthermore, reduces the very approximate description of dispersion effects by the semilocal DF.

The parameter optimization procedure is based on the fit set introduced in Section 4.1. The root-mean-square deviation (rmsd) for the complete fit set is calculated in each fitting cycle and is minimized. The, thus, obtained functionals are in the following denoted by the prefix ‘o’, which stands for optimized, while the suffix ‘-D’ indicates the use of the dispersion correction (e.g., oPWLYP-D or oTPSS-D). To investigate the effect of the reoptimization procedure, calculations were also carried out with the original (*meta*-)GGA functionals. Again the empirical dispersion correction was applied, but this time in the originally proposed version, i.e.,  $r_{\text{scal}}^{\text{vdW}} = 1.1$  and the originally determined  $s_6$  parameters: 1.20 (BLYP-D), 0.75 (PBE-D), and 1.00 (TPSS-D).<sup>41</sup> So far, no  $s_6$  parameter for the mPWLYP functional has been published. Therefore, we determined it by calculations of the S22 test set (def2-QZVP basis). The optimal  $s_6$  parameter was found to be 0.90, which yielded the lowest MAD of 0.60 kcal mol<sup>-1</sup>. B3LYP-D and B2PLYP-D calculations were carried out with the original  $s_6$  values of 1.05 and 0.55, respectively.<sup>31,41</sup>

## 4. Reoptimization of Common (*meta*-)GGA Functionals

**4.1. The Fit Set.** The database used for the fitting procedure consists of 143 entries, comprising seven different chemical properties. The complete set is shown in Table S25 of the Supporting Information. All reference data are ZPVE exclusive and without thermal corrections. The first 49 entries are atomization energies and 47 of them are taken from the G2/97 test set.<sup>1</sup> In addition to the 47 mentioned G2/97 systems, the total atomization energies of the adamantane and anthracene molecules, derived from experiment,<sup>97</sup> are included. These hydrocarbons have about the same size, but the uniformly accurate description of their unsaturated and saturated structures is difficult to achieve by DFs. The next 15 entries are total atomic energies.<sup>98</sup> As these energies are rather large, we scaled down the deviations between the investigated method and the reference data in order to be compatible with the other relative energies (see Table S25, Supporting Information). The fit set includes, furthermore, eight atomic ionization potentials and seven atomic electron affinities taken from the G2-1 test set.<sup>17</sup> As already mentioned above, density functional methods sometimes fail to correctly predict isomerization energies. Therefore, we included the difficult isomerization reaction from isooctane to *n*-octane, which is also part of the ISO34 database, with a weighting factor of 5. As the fitting procedure is carried out with the empirical dispersion correction, it was also important to include noncovalently bound systems. Therefore, we took the five smallest systems from the S22 database. These are the ammonia, water, formic acid, methane, and ethene dimers. Deviations from the reference values are scaled by 20 for the first 3 and by 30 for the last 2 systems. Finally, we included 58 decomposition energies from the MB08-165 subset, which involves rather small but still complicated artificial structures.

**Table 2.** Original and Reoptimized Parameters of the BLYP-D Functional

	$\beta_{\text{B88}}$	$a_{\text{LYP}}$	$b_{\text{LYP}}$	$c_{\text{LYP}}$	$d_{\text{LYP}}$	rmsd <sup>a</sup>
BLYP-D <sup>b</sup>	0.00420	0.04918	0.132	0.2533	0.349	10.01
oBLYP-D <sup>b</sup>	0.00401	0.05047	0.140	0.2196	0.363	8.26

<sup>a</sup> Root mean square deviation for the complete fit set in kcal mol<sup>-1</sup>. All calculations were carried out with (aug)-def2-QZVP. <sup>b</sup>  $s_6 = 1.00$  and  $r_{\text{scal}}^{\text{vdW}} = 1.15$ .

The fitting procedure itself was already outlined in the Computational Details Section. In the following, each reoptimized functional will be discussed.

**4.2. The oBLYP-D Functional.** The BLYP functional consists of Becke1988 (B88) exchange<sup>65</sup> combined with LYP correlation. The expression for B88 exchange is<sup>65</sup>

$$E_X^{\text{B88}} = E_X^{\text{LDA}} - \beta_{\text{B88}} \sum_{\sigma} \int \rho_{\sigma}^{4/3} \frac{x_{\sigma}^2}{1 + 6\beta_{\text{B88}} x_{\sigma} \sinh^{-1} x_{\sigma}} d^3r \quad (5)$$

where  $E_X^{\text{LDA}}$  is the LDA exchange energy,  $\sigma$  is the spin variable (for  $\alpha$  and  $\beta$  spin, respectively), and  $x_{\sigma}$  is the reduced gradient variable, defined in eq 6:

$$x_{\sigma} = \frac{|\nabla \rho_{\sigma}|}{\rho_{\sigma}^{4/3}} \quad (6)$$

The parameter  $\beta_{\text{B88}}$  was originally obtained by a fit to the Hartree–Fock exchange energies of the six rare gas atoms from He to Rn. It was determined to be 0.00420 au (see Table 2).

Lee, Yang, and Parr derived the LYP correlation functional as a second-order gradient expansion of the Colle–Salvetti formula.<sup>66,69</sup> Miehlich et al. eliminated the second-order gradient from the LYP formula by partial integration and presented the following expression, which is usually implemented in DFT program packages (eq 7):<sup>100</sup>

$$E_C^{\text{LYP}} = -a_{\text{LYP}} \int \frac{4}{1 + d_{\text{LYP}} \rho^{-1/3}} \frac{\rho_{\alpha} \rho_{\beta}}{\rho} - a_{\text{LYP}} b_{\text{LYP}} \int \omega \{ \rho_{\alpha} \rho_{\beta} [2^{11/3} C_F (\rho_{\alpha}^{8/3} + \rho_{\beta}^{8/3}) + (\frac{47}{18} - \frac{7}{18} \delta) |\nabla \rho|^2 - (\frac{5}{2} - \frac{1}{18} \delta) (|\nabla \rho_{\alpha}|^2 + |\nabla \rho_{\beta}|^2) - \frac{\delta - 11}{9} (\frac{\rho_{\alpha}}{\rho} |\nabla \rho_{\alpha}|^2 + \frac{\rho_{\beta}}{\rho} |\nabla \rho_{\beta}|^2)] - \frac{2}{3} \rho^2 |\nabla \rho|^2 + (\frac{2}{3} \rho^2 - \rho_{\alpha}^2) |\nabla \rho_{\beta}|^2 + (\frac{2}{3} \rho^2 - \rho_{\beta}^2) |\nabla \rho_{\alpha}|^2 \} \quad (7)$$

with

$$\omega = \frac{\exp(-c_{\text{LYP}} \rho^{-1/3})}{1 + d_{\text{LYP}} \rho^{-1/3}} \rho^{-11/3}, \quad \delta = c_{\text{LYP}} \rho^{-1/3} + \frac{d_{\text{LYP}} \rho^{-1/3}}{1 + d_{\text{LYP}} \rho^{-1/3}}, \quad C_F = \frac{3}{10} (3\pi^2)^{2/3} \quad (8)$$

**Table 3.** Original and Reoptimized Parameters of the mPWLYP-D Functional

	$b_{PW}$	$c_{PW}$	$d_{PW}$	$a_{LYP}$	$b_{LYP}$	$c_{LYP}$	$d_{LYP}$	rmsd <sup>a</sup>
mPWLYP-D <sup>b</sup>	0.00426	1.6455	3.72	0.04918	0.132	0.2533	0.349	8.99
oPWLYP-D <sup>b</sup>	0.00402	0.8894	0.79	0.04960	0.144	0.2262	0.346	8.26

<sup>a</sup> Rmsd for the complete fit set in kcal mol<sup>-1</sup>. All calculations were carried out with (aug)-def2-QZVP. <sup>b</sup>  $s_6 = 1.00$  and  $r_{scal}^{vdW} = 1.15$ .

The LYP functional depends on four parameters  $a_{LYP}$ ,  $b_{LYP}$ ,  $c_{LYP}$ , and  $d_{LYP}$  that were determined from a fit to the He atom (see Table 2).

An evaluation of the BLYP-D functional with the original parameters and the modified dispersion correction ( $s_6 = 1.00$  and  $r_{scal}^{vdW} = 1.15$ ) gave an rmsd of 10.01 kcal mol<sup>-1</sup>. During the fitting procedure, the rmsd was reduced by 17% and was converged to a value of 8.26 kcal mol<sup>-1</sup>. The optimal parameters of the new oBLYP-D functional are also shown in Table 2. A reduction of the parameter values  $\beta_{B88}$  and  $b_{LYP}$  is observed, while the other values increased.

**4.3. The oPWLYP-D Functional.** The Perdew–Wang (PW) exchange<sup>101</sup> can be regarded as an enhanced form of B88 exchange, that additionally fulfills the Levy condition<sup>102</sup> and the Lieb–Oxford bound.<sup>103</sup> Its expression is shown in eq 9:

$$E_X^{mPW} = E_X^{LDA} - \sum_{\sigma} \int \rho_{\sigma}^{4/3} \frac{b_{PW} x_{\sigma}^2 - (b_{PW} - \beta) x_{\sigma}^2 \exp(-c_{PW} x_{\sigma}^2) - 10^{-6} x_{\sigma}^{d_{PW}}}{1 + 6b_{PW} x_{\sigma} \sinh^{-1} x_{\sigma} - \frac{10^{-6} x_{\sigma}^{d_{PW}}}{A_x}} d^3r \quad (9)$$

with

$$\beta = 5(36\pi)^{-5/3}, \quad A_x = -\frac{3}{2} \left( \frac{3}{4\pi} \right)^{1/3} \quad (10)$$

It depends on three parameters  $b_{PW}$ ,  $c_{PW}$ , and  $d_{PW}$ . In order to enlarge the applicability of the PW functional, Adamo and Barone proposed an adjustment of these three parameters, leading to the modified Perdew–Wang exchange functional (mPW).<sup>61</sup> This adjustment was carried out as a fit to exact exchange energies of isolated atoms and to the differential exchange energies of the helium and neon dimers near their vdWs minima. These adjusted parameters are given in Table 3.

We started our reoptimization of the parameters with the mPWLYP-D functional, that yields an rmsd of 8.99 kcal mol<sup>-1</sup>. Interestingly, the fitting procedure did not improve the rmsd value as much as for BLYP-D. In fact, the final rmsd value of the optimized PWLYP-D functional (oPWLYP-D) is exactly the same as that of oBLYP-D (8.26 kcal mol<sup>-1</sup>).

All three parameter values of the exchange part were reduced. The final value of  $b_{PW}$  is almost the same as for  $\beta_{B88}$  in oBLYP-D (0.00402 compared to 0.00401 au). The value of  $c_{PW}$  was reduced by about 50%. The impact of the fitting procedure, though, is largest for the parameter  $d_{PW}$ . Its value decreased from 3.72 to 0.79. (Table 3). Adamo and Barone argued that this parameter is of particular importance for the long-range behavior of the functional. The observed large decrease can, thus, be explained by the fact that the

dispersion correction was applied throughout the fitting process, therefore, reducing the long-range influence inherent in the mPW functional. Due to the strongly reduced parameter values for  $c_{PW}$  and  $d_{PW}$  and the fact that  $b_{PW}$  has a similar value to  $\beta_{B88}$  of the reoptimized B88 exchange, we can conclude that the reoptimized PW exchange became more ‘B88-like’. Evidence for this are the identical rmsd values for both oBLYP-D and oPWLYP-D.

The changes in the four LYP parameter values show similar tendencies as for the combination with B88 exchange, with the exception that here  $d_{LYP}$  also decreases. The exact values, though, are different than for oBLYP-D. All values of the new oPWLYP-D functional are shown in Table 3.

**4.4. The oPBE-D Functional.** The PBE exchange functional has the following form (eq 11) in which  $\epsilon_X^{LDA}$  is the LDA exchange energy density and  $F_X^{PBE}(s)$  the PBE enhancement factor (eq 12):<sup>43</sup>

$$E_X^{PBE} = \sum_{\sigma} \int \rho \epsilon_X^{LDA} F_X^{PBE}(s_{\sigma}) d\mathbf{r} \quad (11)$$

$$F_X^{PBE}(s) = 1 + \kappa_{PBE} - \frac{\kappa_{PBE}}{1 + \frac{\mu_{PBE} s_{\sigma}^2}{\kappa_{PBE}}} \quad (12)$$

$\kappa_{PBE}$  and  $\mu_{PBE}$  are functional parameters and  $s_{\sigma} = x_{\sigma}/2(3\pi^2)^{1/3}$ .

The correlation portion of the PBE functional can be written as a gradient expansion based on the correlation energy density of the uniform electron gas  $\epsilon_C^{LDA}$  (using its PW parametrization) and on another reduced gradient variable  $t_{\sigma}$  (eqs 13 and 14):

$$E_C^{PBE} = \sum_{\sigma} \int \rho (\epsilon_C^{LDA} + \beta_{PBE} t_{\sigma}^2 + \dots) d\mathbf{r} \quad (13)$$

with

$$t_{\sigma} \propto \frac{|\nabla \rho_{\sigma}|}{\phi(\xi) \rho_{\sigma}}, \quad \phi(\xi) = \frac{(1 + \xi)^{2/3} + (1 - \xi)^{2/3}}{2}, \quad \xi = \frac{\rho_{\alpha} - \rho_{\beta}}{\rho} \quad (14)$$

The parameter  $\beta_{PBE}$  controls the amount of gradient correction to the LDA part.

The original parameter values for  $\kappa_{PBE}$ ,  $\mu_{PBE}$ , and  $\beta_{PBE}$  are shown in Table 4. Several modifications of these were already published in the past and showed the sensitivity of the functional’s results toward the parameters’ values. Examples are the revised functionals revPBE,<sup>52</sup> RPBE,<sup>53</sup> mPBE,<sup>54</sup> PBEsol,<sup>55</sup> and other variants.<sup>56,57</sup>

When employing the PBE-D functional with the modified empirical dispersion correction (with  $s_6$  and  $r_{scal}^{vdW}$  defined above), the rmsd for the complete fit set is very large with

**Table 4.** Original and Reoptimized Parameters of the PBE-D Functional

	$\kappa_{\text{PBE}}$	$\mu_{\text{PBE}}$	$\beta_{\text{PBE}}$	rmsd <sup>a</sup>
PBE-D <sup>b</sup>	0.8040	0.21952	0.06672	17.11
oPBE-D <sup>b</sup>	1.2010	0.21198	0.04636	9.02

<sup>a</sup> Rmsd for the complete fit set in kcal mol<sup>-1</sup>. All calculations were carried out with (aug)-def2-QZVP. <sup>b</sup>  $s_6 = 1.00$  and  $r_{\text{scal}}^{\text{vdW}} = 1.15$ .

17.11 kcal mol<sup>-1</sup>. The reparameterization gave an rmsd of 9.02 kcal mol<sup>-1</sup>, which means a reduction of about 50%. The optimized parameter values are also shown in Table 4. A strong increase for  $\kappa_{\text{PBE}}$  can be observed. The final value is 1.2010, i.e., similar to that of revPBE (1.245).<sup>52</sup> The other two parameter values ( $\mu_{\text{PBE}}$  and  $\beta_{\text{PBE}}$ ) decrease.

**4.5. The oTPSS-D Functional.** Based on the PBE functional, Perdew, Kurth, Zupan, and Blaha derived a new meta-GGA functional called PKZB.<sup>104</sup> Further adjustments to PKZB were then undertaken by Tao, Perdew, Staroverov, and Scuseria resulting in the TPSS functional.<sup>44</sup>

The exchange part of the functional is similar to that of PBE in eq 11, but a new enhancement factor  $F_X^{\text{TPSS}}$  is defined (eq 15):

$$F_X^{\text{TPSS}} = 1 + \kappa_{\text{PBE}} - \frac{\kappa_{\text{PBE}}}{1 + \frac{x}{\kappa_{\text{PBE}}}} \quad (15)$$

$\kappa_{\text{PBE}}$  is the same as for PBE. The variable  $x$  is given as (eq 16):

$$x = \left\{ \left[ \frac{10}{81} + c_{\text{TPSS}} \frac{z^2}{(1+z^2)^2} \right] p + \frac{146}{2025} \tilde{q}_b^2 - \frac{73}{405} \tilde{q}_b \sqrt{\frac{1}{2} \left( \frac{3}{5} z \right)^2 + \frac{1}{2} p^2} + \frac{1}{\kappa_{\text{PBE}}} \left( \frac{10}{81} \right)^2 p^2 + 2 \sqrt{e_{\text{TPSS}} \frac{10}{81} \left( \frac{3}{5} z \right)^2 + e_{\text{TPSS}} \mu_{\text{PBE}} p^3} \right\} / [(1 + \sqrt{e_{\text{TPSS}} p})^2] \quad (16)$$

where

$$\begin{aligned} z &= \frac{\tau^W}{\tau} & \alpha &= \frac{\tau - \tau^W}{\tau^{\text{UEG}}} \\ \tilde{q}_b &= \frac{9}{20} \frac{(\alpha - 1)}{[1 + b_{\text{TPSS}} \alpha (\alpha - 1)]^{1/2}} + \frac{2p}{3} \end{aligned} \quad (17)$$

$p$  is  $s^2$ ,  $\tau$  the kinetic energy density,  $\tau^W$  the von Weizsäcker kinetic energy density, and  $\tau^{\text{UEG}}$  the uniform gas kinetic energy density. The  $\mu_{\text{PBE}}$  parameter is the same as for PBE;  $b_{\text{TPSS}}$ ,  $c_{\text{TPSS}}$ , and  $e_{\text{TPSS}}$  are new functional parameters (see Table 5).

The TPSS correlation functional is defined as follows (eq 18):

$$E_C^{\text{TPSS}} = \int \rho \varepsilon_C^{\text{revPKZB}} \left[ 1 + d_{\text{TPSS}} \varepsilon_C^{\text{revPKZB}} \left( \frac{\tau^W}{\tau} \right)^3 \right] d^3r \quad (18)$$

with

$$\begin{aligned} \varepsilon_C^{\text{revPKZB}} &= \varepsilon_C^{\text{PBE}} [\rho_\alpha, \rho_\beta, \nabla \rho_\alpha, \nabla \rho_\beta] \left[ 1 + C(\zeta, \xi) \left( \frac{\tau^W}{\tau} \right)^2 \right] - \\ &\quad [1 + C(\zeta, \xi)] \left( \frac{\tau^W}{\tau} \right)^2 \sum_\sigma \frac{\rho_\sigma}{\rho} \tilde{\varepsilon}_C \quad (19) \end{aligned}$$

where

$$\begin{aligned} \tilde{\varepsilon}_C &= \max[\varepsilon_C^{\text{PBE}}[\rho_\sigma, 0, \nabla \rho_\sigma, 0], \varepsilon_C^{\text{PBE}}[\rho_\alpha, \rho_\beta, \nabla \rho_\alpha, \nabla \rho_\beta]] \\ C(\zeta, \xi) &= \frac{0.53 + 0.87\zeta^2 + 0.50\zeta^4 + 2.26\zeta^6}{\left[ 1 + \xi^2 \frac{(1+\zeta)^{-4/3} + (1-\zeta)^{-4/3}}{2} \right]^4} \\ \xi &= \frac{|\nabla \zeta|}{2(3\pi^2\rho)^{1/3}} \end{aligned} \quad (20)$$

As defined in eq 14,  $\zeta$  is the relative spin polarization. The TPSS correlation part depends on two parameters. These are  $d_{\text{TPSS}}$ , as shown in eq 18, and  $\beta_{\text{PBE}}$ , which is part of the PBE correlation functional  $\varepsilon_C^{\text{PBE}}$  and of  $\tilde{\varepsilon}_C$  (ref 44 gives a detailed description of all the necessary variables in the TPSS functional). In 2007, Perdew et al. published a reparameterized version of TPSS, with different values for  $\mu_{\text{PBE}}$ ,  $c_{\text{TPSS}}$ , and  $e_{\text{TPSS}}$  (Table 5).<sup>58</sup> In this study, we will refer to this modified variant as ‘mod-TPSS’. Very recently, another revised version of TPSS (revTPSS) was presented.<sup>59</sup>

In total, we chose to optimize seven parameters as shown in Table 5. Initially, TPSS-D yielded an rmsd of 9.69 kcal mol<sup>-1</sup>, which was reduced by about 30% to 6.81 kcal mol<sup>-1</sup>. This is the lowest rmsd obtained for the fit set in this study. Lifting all physical constraints, that were imposed on the original derivation of TPSS, has a great influence on all seven parameter values (see Table 5). In particular,  $b_{\text{TPSS}}$ ,  $e_{\text{TPSS}}$ , and  $d_{\text{TPSS}}$  change significantly. The original PBE parameters show the opposite trend for oTPSS-D than for oPBE-D, i.e.,  $\kappa_{\text{PBE}}$  decreases, whereas  $\mu_{\text{PBE}}$  and  $\beta_{\text{PBE}}$  strongly increase.

## 5. Results and Discussion

**5.1. The GMTKN24 Set.** **5.1.1. oBLYP-D and oPWLYP-D.** The MADs for all subsets of the GMTKN24 database are shown for the BLYP-D and oBLYP-D functionals in Figure 2. The actual MAD and the rmsd values for these functionals with and without dispersion correction are shown in Tables S26 and S27 of the Supporting Information. Reparameterizing the functional lowers the MAD for the MB08–165 subset by 1 kcal mol<sup>-1</sup> (from 9.2 to 8.2 kcal mol<sup>-1</sup>). Atomization energies, on the other hand, are better described by the original parameters (the MAD increases by about 1 kcal mol<sup>-1</sup> for oBLYP-D). Ionization potentials and electron affinities are not affected by the reparameterization. Proton affinities are slightly better described by 0.4 kcal mol<sup>-1</sup> with oBLYP-D. The effect of the reparameterization on SIE related problems either is negligible (see the almost identical MADs for BHPERI) or leads to slightly worse results: the MADs for the SIE11 and BH76 sets increase by 0.5 kcal mol<sup>-1</sup> each.

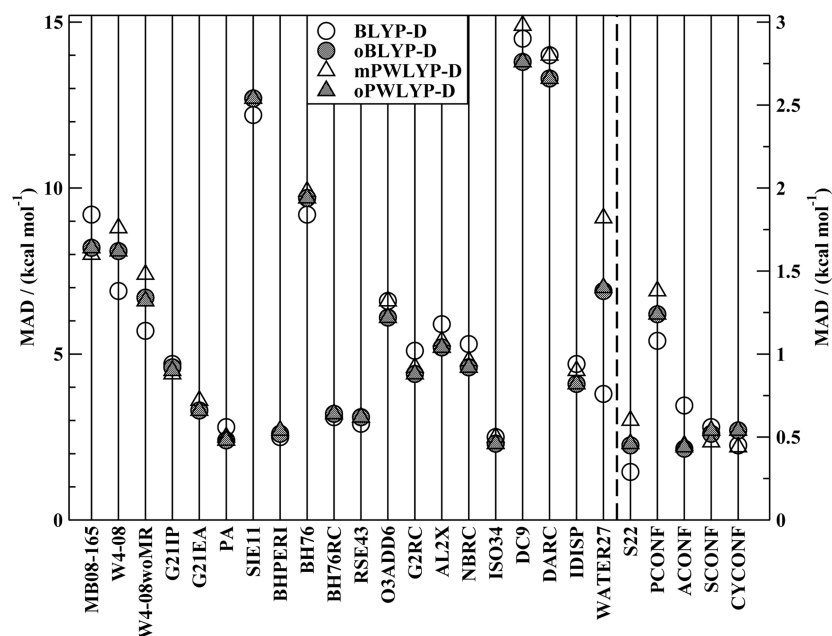
The impact of the new parameters on reaction energies depends on their type. Whereas the values for the BH76RC,



**Table 5.** Original and Reoptimized Parameters of the TPSS-D Functional

	$b_{\text{TPSS}}$	$c_{\text{TPSS}}$	$e_{\text{TPSS}}$	$\mu_{\text{PBE}}$	$\kappa_{\text{PBE}}$	$\beta_{\text{PBE}}$	$d_{\text{TPSS}}$	rmsd <sup>a</sup>
TPSS-D <sup>b</sup>	0.40	1.59096	1.537	0.21952	0.804	0.06672	2.8	9.69
'modTPSS' <sup>c</sup>	0.40	1.39660	1.380	0.25000	0.804	0.06672	2.8	—
oTPSS-D <sup>b</sup>	3.43	0.75896	0.165	0.41567	0.778	0.08861	0.7	6.81

<sup>a</sup> Rmsd for the complete fit set in kcal mol<sup>-1</sup>. All calculations were carried out with (aug)-def2-QZVP. <sup>b</sup>  $s_6 = 1.00$  and  $r_{\text{vdW}}^{\text{rdW}} = 1.15$ .  
<sup>c</sup> Modified TPSS variant taken from ref 58. No rmsd value was calculated for this functional.

**Figure 2.** MADs of the (o)BLYP-D and o/mPWLYP-D methods for the GMTKN24 benchmark set. For a better visualization, a different scale is used for the last five data sets. All calculations were carried out with (aug)-def2-QZVP.

RSE43, and ISO34 sets do not change much, improvements for oBLYP-D can be observed for O3ADD6 (improvement by 0.5 kcal mol<sup>-1</sup>), G2RC, AL2X, and NBRC (0.7 kcal mol<sup>-1</sup>, each). The MADs for the difficult cases (DC9) and Diels–Alder reactions (DARC) also decrease, although they are still at a high level with 13.8 and 13.3 kcal mol<sup>-1</sup>, respectively.

The description of intramolecular dispersion effects improves (from 4.7 to 4.1 kcal mol<sup>-1</sup>). For the WATER27 set, though, a peculiar behavior is observed. The MAD value increases from 3.8 to 6.9 kcal mol<sup>-1</sup>. On the contrary, oBLYP without dispersion correction shows an MAD of 4.1 kcal mol<sup>-1</sup> (compared to 9.9 kcal mol<sup>-1</sup> for BLYP). This can be primarily attributed to the large (H<sub>2</sub>O)<sub>20</sub> clusters that contain many hydrogen bonds. When applying the dispersion correction to such systems, the results are very prone to the scale parameter of the vdW radii. On the other hand, the chosen functional also seems to be important, and compensating effects between functional and dispersion correction cannot be always foreseen. Another example is the S22 test set for which the original BLYP-D shows an extraordinary good result (MAD of 0.29 kcal mol<sup>-1</sup>), which is in the range of double-hybrid functionals (see Tables S26 and S35 in the Supporting Information). The oBLYP-D method yields an MAD of 0.45 kcal mol<sup>-1</sup>, which is worse than BLYP-D but still a good result compared to other functionals.

The four conformer subsets benefit for both BLYP and oBLYP from the dispersion correction. But for these sets, a heterogeneous behavior can be observed. While the values

increase for PCONF (by 0.14 kcal mol<sup>-1</sup>) and CYCONF (by 0.09 kcal mol<sup>-1</sup>), ACONF and SCONF are better described by oBLYP-D (by 0.26 and 0.04 kcal mol<sup>-1</sup>).

The mPWLYP-D and oPWLYP-D functionals (Figure 2 and Tables S28 and S29 in the Supporting Information) show a different behavior. The MAD of mPWLYP-D for MB08–165 is already very good for a GGA functional with 8.0 kcal mol<sup>-1</sup>. It worsens slightly by 0.2 kcal mol<sup>-1</sup> for oPWLYP-D. For most of the subsets, the MAD almost stays the same when changing the parameters. Improvements are observed for atomization energies (by 0.6 kcal mol<sup>-1</sup>), O3ADD6 (0.5 kcal mol<sup>-1</sup>), DC9 (1.1 kcal mol<sup>-1</sup>), DARC (0.7 kcal mol<sup>-1</sup>), IDISP (0.4 kcal mol<sup>-1</sup>), WATER27 (2.1 kcal mol<sup>-1</sup>), and S22 (by 0.14 kcal mol<sup>-1</sup>). The description of conformers improves slightly for PCONF, does not change at all for ACONF, and worsens slightly for SCONF and CYCONF.

A direct comparison between BLYP-D and mPWLYP-D clearly shows that in some cases both functionals differ significantly from each other, while in others they show similar results. The reparameterization, though, has the effect that both, oBLYP-D and oPWLYP-D yield almost identical MADs for all 24 subsets. This underlines the statement already made in the previous section, that the PW exchange part became more ‘B88-like’, and that a mathematically simpler functional performs almost identically to a more complicated one.

**5.1.2. oPBE-D and oTPSS-D.** The behavior of PBE-D and oPBE-D is more heterogeneous than for the functionals discussed above (Figure 3 and Tables S30 and S31 in the

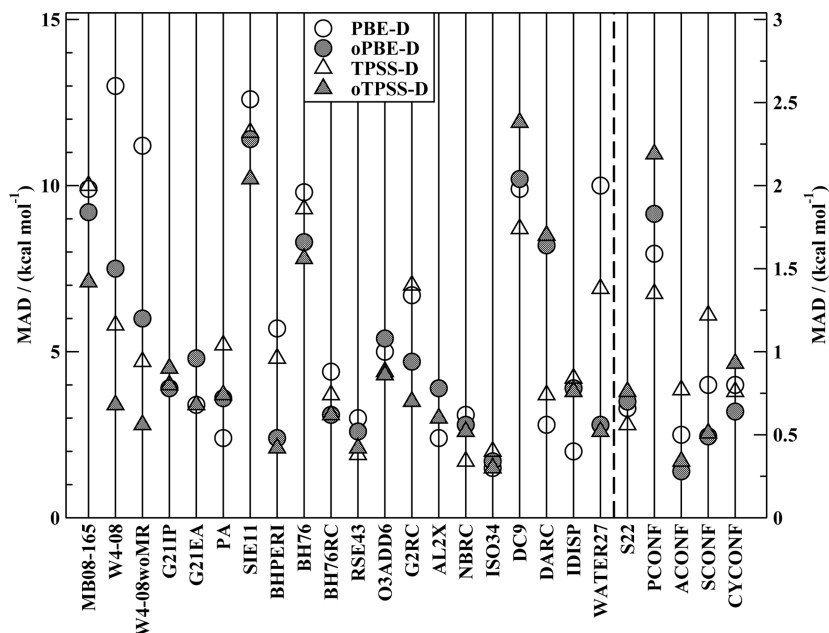


**Figure 3.** MADs of the (o)PBE-D and (o)TPSS-D methods for the GMTKN24 benchmark set. For a better visualization, a different scale is used for the last five data sets. All calculations were carried out with (aug)-def2-QZVP.

Supporting Information). In many cases, oPBE-D performs better than PBE-D. The MAD for the MB08–165 subset decreases by 0.7 to 9.2 kcal mol<sup>−1</sup>, although this value is still 1 kcal mol<sup>−1</sup> higher than for oBLYP-D. A large improvement is observed for atomization energies, which is in accordance with the parameter value of  $\kappa_{\text{PBE}}$  becoming more ‘revPBE-like’. The MAD for W4–08 is reduced by more than 40% from 13.0 to 7.4 kcal mol<sup>−1</sup>. The MAD for the SIE11 test set is reduced by 1.2 kcal mol<sup>−1</sup>. A closer look at the barrier height subsets reveals that the original PBE-D approach shows worse results than the BLYP-D functional (e.g., 5.7 compared to 2.5 kcal mol<sup>−1</sup> for BHPERI and 9.8 vs 9.2 kcal mol<sup>−1</sup> for BH76). The optimized version though yields better MADs than that of oBLYP-D (2.4 vs 2.6 kcal mol<sup>−1</sup> for BHPERI and 8.3 vs 9.7 kcal mol<sup>−1</sup> for BH76).

Improvements for oPBE-D are also observed for the ‘small molecule’ reaction energy test sets, as can be seen for BH76RC, RSE43, and G2RC. For the latter one, the MAD is 2 kcal mol<sup>−1</sup> lower than for PBE-D. The other reaction subsets show more or less similar results (O3ADD6, NBRC, ISO34, and DC9). This is also the case for the ionization potentials for which neither the dispersion correction nor the reparameterization have any significant effect.

Worse MADs are observed for the description of electron and proton affinities and the AL2X, DARC, and IDISP subsets. For the DARC subset, the very good MAD of 2.8 kcal mol<sup>−1</sup> for PBE-D (better than any other functional in this study) increases by a factor of 3, although the MAD of 8.2 kcal mol<sup>−1</sup> for oPBE-D is still better than those of the other optimized functionals.

For WATER27, the functionals again exhibit a peculiar behavior. Adding the dispersion correction with the originally proposed scale factors leads to an increased MAD from 3.2 (PBE) to 10.0 kcal mol<sup>−1</sup> (PBE-D). The opposite behavior is observed for the optimized functional with different scale factors for the dispersion correction. Here, the MAD for

oPBE is quite large with 12.1 kcal mol<sup>−1</sup>, but it decreases to a very small value of 2.8 kcal mol<sup>−1</sup> for oPBE-D.

The MAD for the S22 set is slightly larger (by 0.04 kcal mol<sup>−1</sup>) for oPBE-D than for PBE-D. The MAD increases also for the tripeptide conformers. On the other hand, the alkane, sugar, and cysteine conformers are much better described by oPBE-D.

Similar trends can also be observed for the TPSS-D and oTPSS-D functionals (Figure 3 and Tables S32 and S33 in the Supporting Information). Although located on a higher rung on Jacob’s Ladder, TPSS-D does not perform better for MB08–165 than the GGA functionals (MAD of 10.0 kcal mol<sup>−1</sup>). On the contrary, oTPSS-D performs very well with 7.1 kcal mol<sup>−1</sup>, which is a value that comes close to that of hybrid functionals. Large improvements are also observed for atomization energies, proton affinities, SIE related problems, and barrier heights and the BH76RC, G2RC, ISO34, and IDISP subsets. On the other hand, MADs worsen for G21IP, NBRC, DC9, and DARC, but only the results for the last two sets can be regarded as ‘outliers’ for the complete database (MADs of 11.9 and 8.5 kcal mol<sup>−1</sup>). The combination of the new functional parameters and slightly modified dispersion correction parameters performs better for IDISP and WATER27. In fact, the MAD of oTPSS-D for WATER27 is with 2.6 kcal mol<sup>−1</sup> the best of all functionals tested in this study. On the other hand, the MAD for the S22 test increases by 0.2 kcal mol<sup>−1</sup>. The description of the tripeptide conformers also deteriorates (1.4 kcal for TPSS-D vs 2.2 kcal mol<sup>−1</sup> for oTPSS-D). The MADs for ACONF and SCONF improve by about 60%. CYCONF, though, shows a slightly worse MAD for oTPSS-D (0.76 vs 0.93 kcal mol<sup>−1</sup>).

Another way to compare the oTPSS-D functional with TPSS-D is shown in Figure 4, part a. There the ratios of the MADs of both functionals [i.e., MAD(oTPSS-D)/MAD(TPSS-D)] are shown. A value smaller than 1 means that oTPSS-D

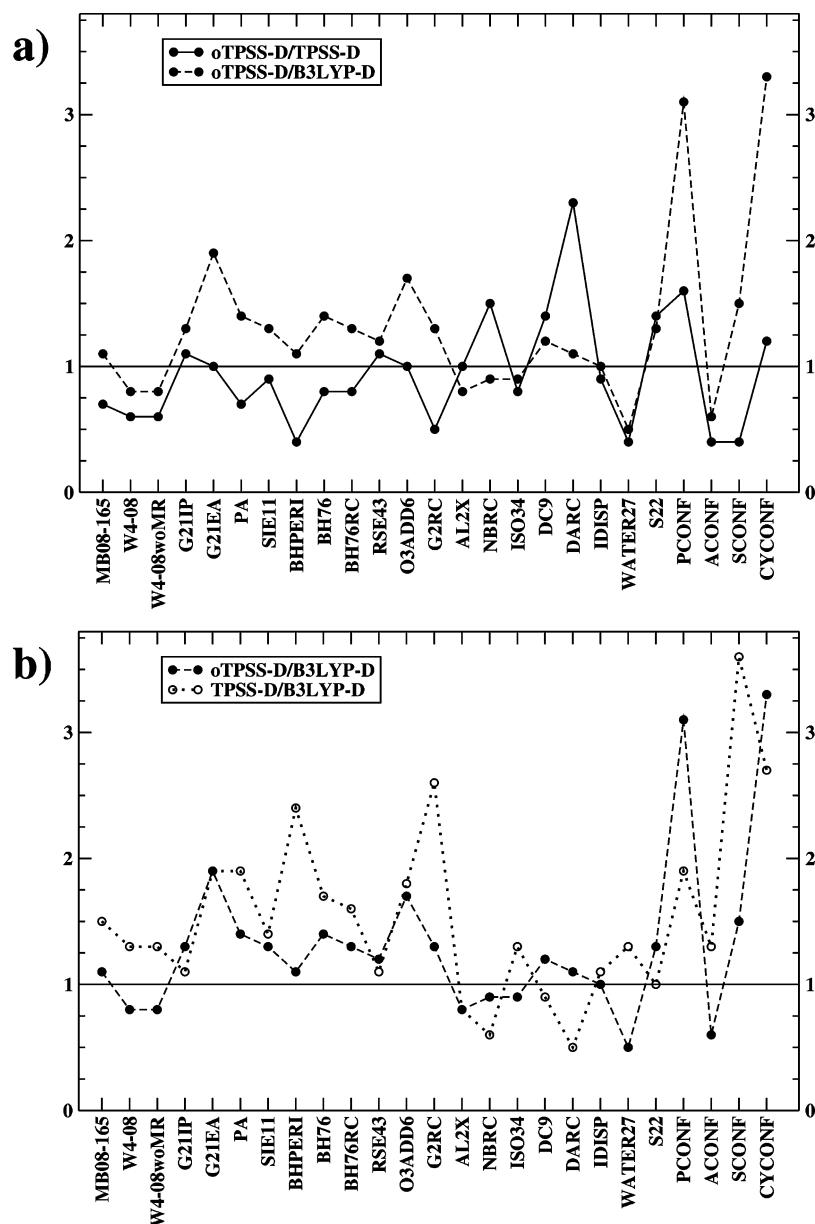


**Figure 4.** Ratios of the MADs of oTPSS-D and TPSS-D (a), oTPSS-D and B3LYP-D (a and b), and TPSS-D and B3LYP-D (b) for the complete GMTKN24 database. The lines between the data points are just drawn to guide the eye.

performs better than TPSS-D and vice versa. Values close to 1 indicate only minor changes. The curve clearly shows the reoptimized functional's improved performance for most of the considered subsets. Additionally, we tested the modified TPSS variant ('modTPSS') by Perdew et al. for the complete GMTKN24 database. The MADs and rmsds are shown in the Supporting Information, Table S34. A comparison between oTPSS-D, TPSS-D, and 'mod-TPSS-D' is shown in Figure S1 in the Supporting Information. It can clearly be seen that 'mod-TPSS-D' often yields results that are similar to TPSS-D and that it is also outperformed by oTPSS-D.

As the TPSS functional belongs to a higher rung on Jacob's Ladder, it is also more expensive than, e.g., PBE, due to the calculation of the kinetic energy density. This increase in computing time, however, is less than the corresponding increase when going to hybrids, and using TPSS would be adequate if its accuracy and robustness were significantly higher than for PBE.

The GMTKN24 database allows a direct comparison between PBE and TPSS, and thus, it is possible to evaluate the cost–benefit ratio for TPSS. In only five cases, the TPSS-D approach shows an improvement of more than 1 kcal mol<sup>-1</sup> compared to that of PBE-D: W4-08, SIE11, RSE43, NBRC, and DC9. In two cases, PBE-D is better by more than 1 kcal mol<sup>-1</sup> (PA and IDISP). In all of the other cases the PBE-D and TPSS-D results lie close to each other, and there is no real improvement when applying the *meta*-GGA functional.

When comparing the optimized versions with each other, one sees that the number of cases for which the *meta*-GGA functional is, on average, better by more than 1 kcal mol<sup>-1</sup> increases to six: MB08-165, W4-08, G21EA, SIE11, O3ADD6, and G2RC. On the other hand, oPBE-D shows superior behavior only for the DC9 and CYCONF subsets.

**5.1.3. B3LYP-D and B2PLYP-D.** Additional calculations were carried out with the B3LYP-D and B2PLYP-D methods. The results are shown in Figure 5 and in the Supporting



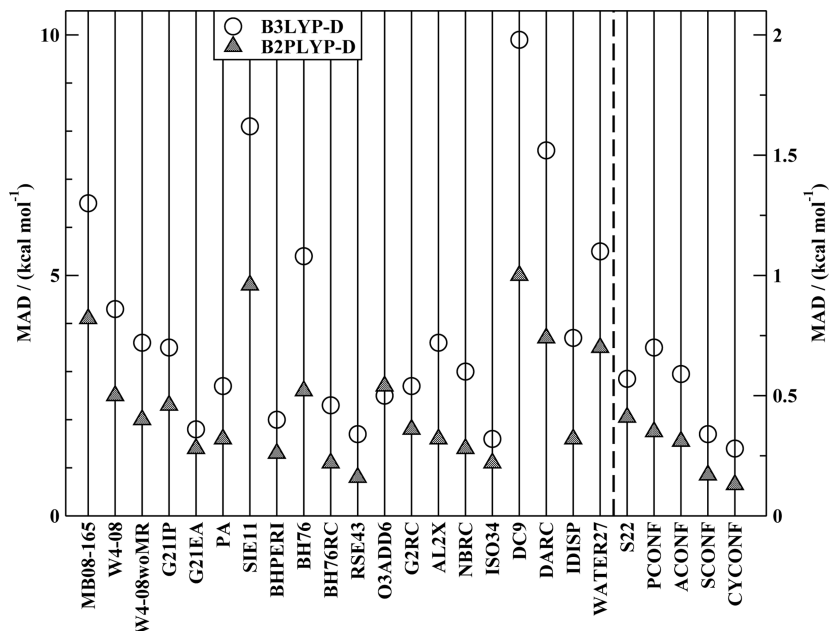


**Figure 5.** MADs of the B3LYP-D and B2PLYP-D methods for the GMTKN24 benchmark set. For a better visualization, a different scale is used for the last five data sets. All calculations were carried out with (aug)-def2-QZVP.

Information, Tables S35 and S36. Not unexpectedly, we find that B2PLYP-D clearly outperforms the allegedly ‘state-of-the-art’ B3LYP functional in all cases. In most of them, the MAD is reduced by 50% or more. Only for G21EA and O3ADD6, the results are quite similar. Both functionals are the only methods in this study that yield an MAD lower than 1 kcal mol<sup>-1</sup> for the PCONF subset (0.70 for B3LYP-D and 0.35 for B2PLYP-D). A comparison between B3LYP-D and the original and optimized (*meta*)-GGA functionals shows that the latter ones sometimes yield better or comparable results. The oTPSS-D functional shows lower or very similar MADs in eight cases: W4-08, BHPERI, AL2X, NBRC, ISO34, IDISP, WATER27, and ACONF. From the results, it can be seen that the other methods also partially outperform B3LYP-D, though not in so many cases as for oTPSS-D (five cases for TPSS-D, seven cases for oPBE-D and PBE-D, and one case for BLYP-D, oBLYP-D, mPWLYP-D, and oPWLYP-D). In Figure 4, the ratios of the MADs of oTPSS-D and B3LYP-D [i.e., MAD(oTPSS-D)/MAD(B3LYP-D)] and of TPSS-D and B3LYP-D [i.e., MAD(TPSS-D)/MAD(B3LYP-D)] are given. The curves clearly show that, in the case of oTPSS-D, the ratios are closer to 1 and in many cases even smaller. On the other hand, the curve for TPSS-D shows that it is by far outperformed by B3LYP-D in the majority of cases.

Compared to B2PLYP-D, better or similar results are obtained for WATER27 (by oTPSS-D and oPBE-D), S22 (by BLYP-D), and ACONF (by oTPSS-D and oPBE-D). Still, B2PLYP-D shows for the majority of cases the best results of all functionals investigated in this study.

**5.1.4. Overall Statistical Analysis.** The analysis of the GMTKN24 database is completed by an overall statistical evaluation. In the spirit of the work by Truhlar and co-workers, we define a weighted total mean absolute deviation (WTMAD) to combine all obtained MADs to one final number for each tested method. Of course, such a value can be defined in several ways, and there is no real right or wrong. We tested many schemes, and the overall interpreta-

tion was not altered by the actual way of calculating the WTMADs. In the scheme, which we finally present here, each of the 24 MAD values is weighted by the number of entries of each subset (see eq 21). This takes into account the size of each set. Furthermore, each subest is weighted by an additional factor that was calculated as the ratio between the MADs of BLYP and B2PLYP-D [i.e., MAD-(BLYP)/MAD(B2PLYP-D)]. This takes into account the difficulty of a certain subset. As one of the worst methods without dispersion correction in this study, BLYP and, as the best method, B2PLYP-D are chosen. The actual values of these scale factors are usually in a range between 2.0 and 3.0 for reaction energies, atomization energies, ionization potentials and proton and electron affinities. They are significantly larger for SIE11, BHPERI, AL2X, NBRC, DC9, and DARC, and for subsets where London dispersion effects are important. The final formula is:

$$\begin{aligned} \text{WTMAD} = & [2.7 \times 165 \times \text{MAD}(\text{MB08-165}) + \\ & 2.8 \times 99 \times \text{MAD}(\text{W4-08}) + \\ & 2.0 \times 36 \times \text{MAD}(\text{G21IP}) + 2.4 \times 25 \times \text{MAD}(\text{G21EA}) + \\ & 1.6 \times 12 \times \text{MAD}(\text{PA}) + 2.4 \times 11 \times \text{MAD}(\text{SIE11}) + \\ & 4.5 \times 26 \times \text{MAD}(\text{BHPERI}) + \\ & 3.2 \times 76 \times \text{MAD}(\text{BH76}) + \\ & 3.0 \times 30 \times \text{MAD}(\text{BH76(RC)}) + \\ & 4.4 \times 43 \times \text{MAD}(\text{RSE43}) + \\ & 2.2 \times 6 \times \text{MAD}(\text{O3ADD6}) + \\ & 3.1 \times 25 \times \text{MAD}(\text{G2RC}) + 7.1 \times 7 \times \text{MAD}(\text{AL2X}) + \\ & 6.8 \times 6 \times \text{MAD}(\text{NBRC}) + 2.9 \times 34 \times \text{MAD}(\text{ISO34}) + \\ & 4.1 \times 9 \times \text{MAD}(\text{DC9}) + 6.2 \times 14 \times \text{MAD}(\text{DARC}) + \\ & 12.9 \times 6 \times \text{MAD}(\text{IDISP}) + \\ & 2.8 \times 27 \times \text{MAD}(\text{WATER27}) + \\ & 11.7 \times 22 \times \text{MAD}(\text{S22}) + \\ & 13.8 \times 10 \times \text{MAD}(\text{PCONF}) + \\ & 3.5 \times 15 \times \text{MAD}(\text{ACONF}) + \\ & 5.2 \times 17 \times \text{MAD}(\text{SCONF}) + \\ & 5.0 \times 10 \times \text{MAD}(\text{CYCONF})] / 2682.5 \quad (21) \end{aligned}$$

**Table 6.** WTMADs for functionals without (DFT) and with dispersion correction (DFT-D)<sup>a</sup>

functional	DFT	DFT-D <sup>b</sup>
BLYP	7.6	5.3
oBLYP	6.8	5.3
mPWLYP	6.8	5.6
oPWLYP	6.8	5.3
PBE	6.2	5.9
oPBE	6.6	4.9
TPSS	5.8	5.0
'modTPSS' <sup>c</sup>	6.3	5.0
oTPSS	5.5	4.0
B3LYP	5.4	3.6
B2PLYP	3.0	2.0

<sup>a</sup> In kcal mol<sup>-1</sup>. All calculations were carried out with (aug)-def2-QZVP. <sup>b</sup> Empirical dispersion correction. For the optimized functionals with  $s_6 = 1.00$  and  $r_{\text{scal}}^{\text{vdW}} = 1.15$ ; for the other functionals with  $r_{\text{scal}}^{\text{vdW}} = 1.1$  and different  $s_6$  values: 1.20 (BLYP-D), 0.90 (mPWLYP-D), 0.75 (PBE-D), 1.00 (TPSS-D and 'mod-TPSS-D'), 1.05 (B3LYP-D) and 0.55 (B2PLYP-D). <sup>c</sup> 'modTPSS' is the modified TPSS variant taken from ref 58.

The WTMADs for all functionals with and without dispersion correction are listed in Table 6. For all methods, one can see the importance of adding the empirical dispersion correction, as the WTMADs are lowered significantly. The only exception is the PBE functional, where the WTMAD stays nearly the same, due to compensation effects. This is mainly due to the typical overbinding behavior of PBE (e.g., for atomization energies or hydrogen bonds), which is further increased by the dispersion correction.

A comparison between the original and reparameterized versions of BLYP-D and mPWLYP-D shows that, overall, the reparameterization does not change the WTMADs significantly. In the case of BLYP-D and oBLYP-D, the WTMADs have identical values (5.3 kcal mol<sup>-1</sup>); the WTMAD of oPWLYP-D is also 5.3 kcal mol<sup>-1</sup> and is just 0.3 kcal mol<sup>-1</sup> lower than that of mPWLYP-D. While the PBE-D functional at 5.9 kcal mol<sup>-1</sup> has a higher WTMAD than the 'LYP-based' ones, oPBE-D yields a value slightly lower than oBLYP-D and oPWLYP-D (4.9 kcal mol<sup>-1</sup>). Thus, all GGA functionals yield WTMADs of about 5 kcal mol<sup>-1</sup> or more. The WTMAD for TPSS-D is 5.0 kcal mol<sup>-1</sup>. This again emphasizes that TPSS-D cannot be regarded as an improvement compared to GGA functionals. This statement is also valid for the modified TPSS variant ('mod-TPSS-D'; WTMAD = 5.0 kcal mol<sup>-1</sup>). The only reparameterized functional with a value significantly smaller than 5.0 kcal mol<sup>-1</sup> is oTPSS-D. With 4.0 kcal mol<sup>-1</sup>, it is even close to B3LYP-D (3.6 kcal mol<sup>-1</sup>). B2PLYP-D shows the lowest WTMAD of all tested functionals with 2.0 kcal mol<sup>-1</sup>, underlining again its superior performance.

**5.2. Benchmark Study of Geometries.** To test the influence of the reparameterization on molecular structures, the original and optimized (*meta*-)GGA functionals were applied to three geometry benchmark sets. The first one contains 36 bond lengths of 31 small molecules containing first-row elements.<sup>105</sup> The second test set comprises 42 bond lengths of 32 small molecules containing second-row elements.<sup>106</sup> The third test set is made up from 24 transition-metal compounds (28 bond lengths).<sup>107,108</sup> All reference values were derived from experiments. Table 7 shows the mean (MD), MAD, rmsd, smallest (min), and largest

deviations (max) for all test sets and functionals. The actual deviations for each molecule are listed in the Supporting Information, Tables S37–S39.

The results for the light element test set indicates that the reparameterization only has a small influence on the MDs, MADs, and rmsds and the error range. BLYP-D and oBLYP-D yield an MAD of 1.2 and 1.1 pm, respectively. Both mPWLYP-D and oPWLYP-D yield geometries of the same quality with MADs of 1.2 pm. Also for the other functionals the MAD does only change marginally: 1.0 pm for PBE-D, 1.2 pm for oPBE-D, 0.8 pm for TPSS-D, and 0.9 pm for oTPSS-D.

The MADs for the heavy element test set are higher than for the first one, but the same trends can be observed as before. There is only a marginal improvement for oBLYP-D and oPWLYP-D, and similar to the GMTKN24 database, both functionals give identical MADs with 2.2 pm. Both oPBE-D and oTPSS-D yield slightly worse results with 2.0 and 1.6 pm compared to 1.6 (PBE-D) and 1.3 pm (TPSS-D).

The errors for the transition-metal test set are in the same range as for the second one. Again, there is only a small improvement for the 'LYP-based' functionals. Compared to its original version, oPBE-D worsens by 0.6 pm. The MAD of oTPSS-D is larger by 0.3 pm compared to that of TPSS-D.

For all test sets, the reparameterization has only a small impact on the quality of the results. In all three cases, the *meta*-GGA functionals yield the best bond lengths.

## 6. Conclusions

In this study, we presented a new benchmark database for applications to general main group thermochemistry, kinetics, and noncovalent interactions (GMTKN24). It is an unprecedented compilation of 24 different, chemically relevant subsets, that either were taken from already existing databases or are presented here for the first time. The new subsets are benchmarks for self-interaction error-related problems (SIE11), barrier heights of pericyclic reactions (BHPERI), reaction energies for small closed-shell molecules (G2RC), reaction sets for ammonia/borane systems (NBRC), intramolecular London dispersion interactions (IDISP) and for cases that are difficult to treat with DFT methods (DC9). Furthermore, new reference data for a set of sugar conformers (SCONF) were presented. The complete set comprises 1.049 single point calculations and 731 reference energies, based on accurate (excluding zero point vibrational energy and thermal corrections) theoretical or experimental data. We additionally suggested a scheme for calculating a weighted total mean absolute deviation (WTMAD) with which we combine the MADs of all subsets to one final statistical number, thus enabling an overall evaluation of each investigated quantum chemical method. We regard this new combination of sets as particularly useful for the evaluation of DFT methods. This was demonstrated by applying common density functionals on the (*meta*-)GGA, hybrid-GGA, and double-hybrid-GGA levels, including the empirical London dispersion correction developed in our group. Furthermore, we carried out a systematic study on the reparameterization of (*meta*-)GGA functionals to investigate the effect of an empirical parameter fitting procedure on the performance for the

**Table 7.** MD, MAD, rmsd, min, and max Deviations for Bond Lengths in pm for the Original and Reoptimized Functionals for Three Test Sets<sup>a</sup>

	BLYP-D	oBLYP-D	mpWLYP-D	oPWLYP-D	PBE-D	oPBE-D	TPSS-D	oTPSS-D
Light Element Test Set <sup>b</sup>								
MD	1.2	1.1	1.2	1.1	1.0	1.2	0.7	0.8
MAD	1.2	1.1	1.2	1.2	1.0	1.2	0.8	0.9
rmsd	1.4	1.3	1.4	1.3	1.2	1.3	1.0	1.2
min	-0.1	-0.2	-0.2	-0.2	-0.6	0.0	-0.5	-1.1
max	3.3	2.8	3.2	2.9	2.8	3.3	2.9	3.2
Heavy Element Test Set <sup>c</sup>								
MD	2.4	2.2	2.3	2.2	1.6	2.0	1.3	1.4
MAD	2.4	2.2	2.3	2.2	1.6	2.0	1.3	1.6
rmsd	2.9	2.6	2.8	2.7	1.8	2.3	1.6	1.9
min	0.3	0.3	0.2	0.4	0.3	0.7	0.1	-1.6
max	7.6	6.3	7.2	6.4	3.4	4.7	4.5	6.0
Transition-Metal Test Set <sup>d</sup>								
MD	2.6	2.3	2.5	2.3	0.7	1.8	0.7	0.3
MAD	2.7	2.4	2.6	2.5	1.5	2.1	1.4	1.7
rmsd	3.2	3.1	3.2	3.1	1.8	2.6	1.8	2.1
min	-1.2	-1.6	-1.3	-1.6	-3.8	-2.6	-3.6	-4.7
max	8.3	9.7	9.1	9.7	3.4	6.2	3.9	3.7

<sup>a</sup> Deviations are defined as theory-experiment. All calculations were carried out with def2-QZVP. The particular  $s_6$  and  $r_{\text{scal}}^{\text{dW}}$  values for each functional can be found in the footnote of Table 6. <sup>b</sup> Experimental data taken from ref 105. <sup>c</sup> Experimental data taken from ref 106. <sup>d</sup> Experimental data taken from refs 107 and 108.

GMTKN24 database and of three different geometry benchmark sets. The refitting was carried out using a fit set containing 143 systems and seven chemically different problems. Our study led to the following conclusions:

- (1) The influence of the new parameters is small for molecular structures (bond lengths). The MADs for the oBLYP-D and oPWLYP-D methods improve by a few tenths of a picometer compared to the original methods. The MADs for oPBE-D and oTPSS-D worsen slightly. As the quality of geometries is not significantly altered, one only has to evaluate the influence of the new parameters on energetics. The reparameterized oBLYP-D version shows, in many cases, slight improvements compared to that of the original functional. On the other hand, the MADs of some subsets are worse or remain unchanged. Optimizing the parameters of the mpWLYP-D functional led to the oPWLYP-D functional, which yields results almost identical to oBLYP-D. The optimized PW-exchange seems to be more 'B88-like'. In the case of oPBE-D (which is more 'revPBE-like') and oTPSS-D, the influence of the new parameters is stronger than for oBLYP-D and oPWLYP-D. The description of many subsets is improved, as shown for the 'mindless-benchmark' set, atomization energies, barrier heights, some reaction energies, water clusters, and relative energies of alkane and sugar conformers. On the other hand, this study also shows that reaching a homogeneous, well-balanced behavior by just refitting existing functionals is difficult, as the description of other properties worsened, like for proton affinities, difficult cases for DFT, the description of Diels-Alder reactions, and relative energies of tripeptide and cysteine conformers.
- (2) A comparison between the B3LYP-D and B2PLYP-D results for the GMTKN24 set shows that the double-hybrid exhibits superior performance by halving the

MADs of B3LYP-D and by yielding the best results for the majority of subsets.

- (3) An analysis of the WTMADs shows that including the empirical dispersion correction is crucial and that it reduces the values by about 1 kcal mol<sup>-1</sup> or more, in most cases. The reparameterization has a small influence on the GGA functionals. The WTMADs are all around 5 kcal mol<sup>-1</sup>. The TPSS-D method is in the same range, whereas a significant improvement is found for the WTMAD of oTPSS-D, which is comparable to that of B3LYP-D. This clearly indicates that the *meta*-GGA functional benefits most from lifting all physical constraints. B2PLYP-D yields by far the smallest WTMAD value (2.0 kcal mol<sup>-1</sup>).
- (4) oTPSS-D outperforms the GGA functionals, particularly for the MB08-165, W4-08, G21EA, SIE11, O3ADD6, and G2RC subsets. It also shows in eight cases better or comparable performance than B3LYP-D. Only for the DC9, DARC, and PCONF subsets is the applicability significantly worsened compared to that of TPSS-D. The above-discussed WTMAD value also underlines oTPSS-D's good performance, and we can recommend it in general and in particular for the calculation of atomization and reaction energies, electron affinities, ionization potentials, barrier heights, and noncovalent interactions. The very good result for the difficult WATER27 set is also striking. We cannot recommend it for self-interaction error-related problems, but note that it performs better than all other semilocal approximations. Functionals of at least hybrid-GGA quality (including a London dispersion correction) should be applied for the description of tripeptide conformers. Our study seems to be the first one that can confirm on very solid grounds previous statements that *meta*-GGAs can be almost as accurate as hybrid functionals.



- (5) The new GMTKN24 database turned out to be effective for the evaluation of a given density functional's overall performance, and we strongly suggest it in future validation works of new functionals with regards to their applicability to chemically relevant problems. We regard this collection of databases as an open project. Whenever new, promising benchmark sets are proposed, we may consider to add them to our compilation, which will always be actualized (also regarding new density functionals) on our Web site.<sup>67</sup>

**Acknowledgment.** This work was supported by the Fonds der Chemischen Industrie with a scholarship to L.G. We thank G. Csonka for providing us with the new reference data for the  $\beta$ -D-glucopyranose conformers included in the SCONF subset and J. Martin for providing us with preprints of the alkane conformer study. We are also grateful to C. Mück-Lichtenfeld for his technical assistance.

**Supporting Information Available:** All entries and reference data of the GMTKN24 database (Tables S1–S24), all entries of the parameters fit set (Table S25), and all results for the GMTKN24 and geometry benchmark sets (Tables S26–S39 and Figure S1). This material is available free of charge via the Internet at <http://pubs.acs.org>.

## References

- (1) Curtiss, L. A.; Raghavachari, K.; Redfern, P. C.; Pople, J. A. *J. Chem. Phys.* **1997**, *106*, 1063–1079.
- (2) Curtiss, L. A.; Raghavachari, K.; Redfern, P. C.; Pople, J. A. *J. Chem. Phys.* **2000**, *112*, 7374–7383.
- (3) Curtiss, L. A.; Redfern, P. C.; Raghavachari, K. *J. Chem. Phys.* **2005**, *123*, 124107.
- (4) Lynch, B. J.; Truhlar, D. G. *J. Phys. Chem. A* **2003**, *107*, 8996–8999.
- (5) Zhao, Y.; Truhlar, D. G. *J. Phys. Chem. A* **2006**, *110*, 10478–10486.
- (6) Zhao, Y.; Truhlar, D. G. *J. Chem. Theory Comput.* **2005**, *1*, 415–432.
- (7) Zhao, Y.; Truhlar, D. G. *J. Phys. Chem. C* **2008**, *112*, 6860–6868.
- (8) Zhao, Y.; Lynch, B. J.; Truhlar, D. G. *J. Phys. Chem. A* **2004**, *108*, 2715–2719.
- (9) Zhao, Y.; González-García, N.; Truhlar, D. G. *J. Phys. Chem. A* **2005**, *109*, 2012–2018.
- (10) Zhao, Y.; Tishchenko, O.; Gour, J. R.; Li, W.; Lutz, J. J.; Piecuch, P.; Truhlar, D. G. *J. Phys. Chem. A* **2009**, *113*, 5786–5799.
- (11) Zhao, Y.; Truhlar, D. G. *Theor. Chem. Acc.* **2008**, *120*, 215–241.
- (12) Zhao, Y.; Truhlar, D. G. *J. Chem. Theory Comput.* **2009**, *5*, 324–333.
- (13) Jurečka, P.; Sponer, J.; Cerný, J.; Hobza, P. *Phys. Chem. Chem. Phys.* **2006**, *8*, 1985–1993.
- (14) Grimme, S.; Steinmetz, M.; Korth, M. *J. Org. Chem.* **2007**, *72*, 2118–2126.
- (15) Korth, M.; Grimme, S. *J. Chem. Theory Comput.* **2009**, *5*, 993–1003.
- (16) Karton, A.; Tarnopolsky, A.; Lamere, J. F.; Schatz, G. C.; Martin, J. M. L. *J. Phys. Chem. A* **2008**, *112*, 12868–12886.
- (17) Curtiss, L. A.; Raghavachari, K.; Trucks, G. W.; Pople, J. A. *J. Chem. Phys.* **1991**, *94*, 7221–7230.
- (18) Parthiban, S.; Martin, J. M. L. *J. Chem. Phys.* **2001**, *114*, 6014–6029.
- (19) Guner, V.; Khuong, K. S.; Leach, A. G.; Lee, P. S.; Bartberger, M. D.; Houk, K. N. *J. Phys. Chem. A* **2003**, *107*, 11445–11459.
- (20) Ess, D. H.; Houk, K. N. *J. Phys. Chem. A* **2005**, *109*, 9542–9553.
- (21) Grimme, S.; Mück-Lichtenfeld, C.; Würthwein, E.-U.; Ehlers, A. W.; Goumans, T. P. M.; Lammertsma, K. *J. Phys. Chem. A* **2006**, *110*, 2583–2586.
- (22) Dinadayalane, T. C.; Vijaya, R.; Smitha, A.; Sastry, G. N. *J. Phys. Chem. A* **2002**, *106*, 1627–1633.
- (23) Neese, F.; Schwabe, T.; Kossmann, S.; Schirmer, B.; Grimme, S. *J. Chem. Theory Comput.* **2009**, *5*, 3060–3073.
- (24) Johnson, E. R.; Mori-Sánchez, P.; Cohen, A. J.; Yang, W. *J. Chem. Phys.* **2008**, *129*, 204112.
- (25) Piacenza, M.; Grimme, S. *J. Comput. Chem.* **2004**, *25*, 83–99.
- (26) Woodcock, H. L.; Schaefer, H. F., III; Schreiner, P. R. *J. Phys. Chem. A* **2002**, *106*, 11923–11931.
- (27) Schreiner, P. R.; Fokin, A. A.; Pascal, R. A.; de Meijere, A. *Org. Lett.* **2006**, *8*, 3635–3638.
- (28) Lepetit, C.; Chermette, H.; Gicquel, M.; Heully, J.-L.; Chauvin, R. *J. Phys. Chem. A* **2007**, *111*, 136–149.
- (29) Lee, J. S. *J. Phys. Chem. A* **2005**, *109*, 11927–11932.
- (30) Grimme, S. *J. Chem. Phys.* **2006**, *124*, 034108.
- (31) Schwabe, T.; Grimme, S. *Phys. Chem. Chem. Phys.* **2007**, *9*, 3397–3406.
- (32) Grimme, S. *Angew. Chem., Int. Ed.* **2006**, *45*, 4460–4464.
- (33) Bryantsev, V. S.; Diallo, M. S.; van Duin, A. C. T.; Goddard III, W. A. *J. Chem. Theory Comput.* **2009**, *5*, 1016–1026.
- (34) Řeha, D.; Valdes, H.; Vondrasek, J.; Hobza, P.; Abu-Riziq, A.; Crews, B.; de Vries, M. S. *Chem.—Eur. J.* **2005**, *11*, 6803–6817.
- (35) Gruzman, D.; Karton, A.; Martin, J. M. L. *J. Phys. Chem. A* **2009**, *113*, 11974–11983.
- (36) Csonka, G. I.; French, A. D.; Johnson, G. P.; Stortz, C. A. *J. Chem. Theory Comput.* **2009**, *5*, 679–692.
- (37) Wilke, J. J.; Lind, M. C.; Schaefer III, H. F.; Császár, A. G.; Allen, W. D. *J. Chem. Theory Comput.* **2009**, *5*, 1511–1523.
- (38) Kurth, S.; Perdew, J. P.; Blaha, P. *Int. J. Quantum Chem.* **1999**, *75*, 889–909.
- (39) Becke, A. D. *J. Chem. Phys.* **1993**, *98*, 5648–5652.
- (40) Stephens, P. J.; Devlin, F. J.; Chabalowski, C. F.; Frisch, M. J. *J. Phys. Chem.* **1994**, *98*, 11623–11627.
- (41) Grimme, S. *J. Comput. Chem.* **2006**, *27*, 1787–1799.
- (42) Perdew, J. P.; Ruzsinszky, A.; Tao, J.; Staroverov, V. N.; Scuseria, G. E.; Csonka, G. *J. Chem. Phys.* **2005**, *123*, 62201.
- (43) Perdew, J. P.; Burke, K.; Ernzerhof, M. *Phys. Rev. Lett.* **1996**, *77*, 3865–3868.

- (44) Tao, J.; Perdew, J. P.; Staroverov, V. N.; Scuseria, G. E. *Phys. Rev. Lett.* **2003**, *91*, 146401.
- (45) Boese, A. D.; Doltsinis, N. L.; Handy, N. C.; Sprik, M. *J. Chem. Phys.* **2000**, *112*, 1670–1678.
- (46) Zhao, Y.; Schultz, N. E.; Truhlar, D. G. *J. Chem. Phys.* **2005**, *123*, 161103.
- (47) Zhao, Y.; Schultz, N. E.; Truhlar, D. G. *J. Chem. Theory Comput.* **2006**, *2*, 364–382.
- (48) Zhao, Y.; Truhlar, D. G. *J. Chem. Phys.* **2006**, *125*, 194101.
- (49) Zhao, Y.; Truhlar, D. G. *J. Phys. Chem. A* **2007**, *110*, 13126–13130.
- (50) Zhao, Y.; Truhlar, D. G. *J. Chem. Theory Comput.* **2008**, *4*, 1849–1868.
- (51) Grimme, S.; Schwabe, T. *Phys. Chem. Chem. Phys.* **2006**, *8*, 4398–4401.
- (52) Zhang, Y.; Yang, W. *Phys. Rev. Lett.* **1998**, *80*, 890–890.
- (53) Hammer, B.; Hansen, L. B.; Norskov, J. K. *Phys. Rev. B: Condens. Matter* **1999**, *59*, 7413–7421.
- (54) Adamo, C.; Barone, V. *J. Chem. Phys.* **2002**, *116*, 5933–5940.
- (55) Perdew, J. P.; Ruzsinszky, A.; Csonka, G. I.; Vydrov, O. A.; Scuseria, G. E.; Constantin, L. A.; Zhou, X.; Burke, K. *Phys. Rev. Lett.* **2008**, *100*, 136406.
- (56) Vela, A.; Medel, V.; Trickey, S. B. *J. Chem. Phys.* **2009**, *130*, 244103.
- (57) Thakkar, A. J.; McCarthy, S. P. *J. Chem. Phys.* **2009**, *131*, 134109.
- (58) Perdew, J. P.; Ruzsinszky, A.; Tao, J.; Csonka, G. I.; Scuseria, G. E. *Phys. Rev. A: At., Mol., Opt. Phys.* **2007**, *76*, 042506.
- (59) Perdew, J. P.; Ruzsinszky, A.; Csonka, G. I.; Constantin, L. A.; Sun, J. *Phys. Rev. Lett.* **2009**, *103*, 026403.
- (60) Tognetti, V.; Adamo, V. *J. Phys. Chem. A* **2009**, DOI: 10.1021/jp903672e (accessed Nov 12, 2009).
- (61) Adamo, C.; Barone, V. *J. Chem. Phys.* **1998**, *108*, 664–675.
- (62) Poater, J.; Duran, M.; Solà, M. *J. Comput. Chem.* **2001**, *14*, 1666–1678.
- (63) Graham, D. C.; Menon, A. S.; Goerigk, L.; Grimme, S.; Radom, L. *J. Phys. Chem. A* **2009**, *113*, 9861–9873.
- (64) Perdew, J. P.; Burke, K.; Ernzerhof, M. *Phys. Rev. Lett.* **1998**, *80*, 891.
- (65) Becke, A. D. *Phys. Rev. A: At., Mol., Opt. Phys.* **1988**, *38*, 3098–3100.
- (66) Lee, C.; Yang, W.; Parr, R. G. *Phys. Rev. B: Condens. Matter* **1988**, *37*, 785–789.
- (67) Prof. Stefan Grimme Research Web Site. <http://www.uni-muenster.de/Chemie.oc/grimme/en/index.html>.
- (68) Martin, J. M. L.; de Oliveira, G. *J. Chem. Phys.* **1999**, *111*, 1843–1856.
- (69) Ruzsinszky, A.; Perdew, J. P.; Csonka, G. I.; Vydrov, O. A.; Scuseria, G. E. *J. Chem. Phys.* **2007**, *126*, 104102.
- (70) Mori-Sanchez, P.; Cohen, A. J.; Yang, W. *J. Chem. Phys.* **2006**, *125*, 201102.
- (71) Zhang, Y.; Yang, W. *J. Chem. Phys.* **1998**, *109*, 2604–2608.
- (72) Gritsenko, O.; Ensing, B.; Schipper, P. R. T.; Baerends, E. J. *J. Phys. Chem. A* **2000**, *104*, 8558–8565.
- (73) Bally, T.; Sastry, G. N. *J. Phys. Chem. A* **1997**, *101*, 7923–7925.
- (74) Grimme, S. *J. Chem. Phys.* **2003**, *118*, 9095–9102.
- (75) Schäfer, A.; Huber, C.; Ahlrichs, R. *J. Chem. Phys.* **1994**, *100*, 5829–5835.
- (76) Raghavachari, K.; Trucks, G. W.; Pople, J. A.; Head-Gordon, M. *Chem. Phys. Lett.* **1989**, *157*, 479–483.
- (77) Jurečka, P.; Hobza, P. *Chem. Phys. Lett.* **2002**, *365*, 89–94.
- (78) Halkier, A.; Helgaker, T.; Jørgensen, P.; Klopper, W.; Koch, H.; Olsen, J.; Wilson, A. K. *Chem. Phys. Lett.* **1998**, *286*, 243–252.
- (79) Dunning, T. H., Jr. *J. Chem. Phys.* **1989**, *90*, 1007–1023.
- (80) Zipse, H. *Top. Curr. Chem.* **2006**, *263*, 163–189.
- (81) Gilbert, T. M. *J. Phys. Chem. A* **2004**, *108*, 2550–2554.
- (82) Kendall, R. A.; Dunning, T. H.; Harrison, R. J. *J. Chem. Phys.* **1992**, *96*, 6796–6806.
- (83) Adamo, C.; Barone, V. *J. Chem. Phys.* **1999**, *110*, 6158–6170.
- (84) Repasky, M. P.; Chandrasekhar, J.; Jorgensen, W. L. *J. Comput. Chem.* **2002**, *23*, 1601–1622.
- (85) Sattelmeyer, K. W.; Tirado-Rives, J.; Jorgensen, W. L. *J. Phys. Chem. A* **2006**, *110*, 13551–13559.
- (86) Grimme, S.; Mück-Lichtenfeld, C. *Chem. Phys. Chem.* **2002**, *2*, 207–209.
- (87) Werner, H.-J.; Knowles, P. J.; Lindh, R.; Manby, F. R.; Schütz, M.; Celani, P.; Korona, T.; Rauhut, G.; Amos, R. D.; Bernhardsson, A.; Berning, A.; Cooper, D. L.; Deegan, M. J. O.; Dobbyn, A. J.; Eckert, F.; Hampel, C.; Hetzer, G.; Lloyd, A. W.; McNicholas, S. J.; Meyer, W.; Mura, M. E.; Nicklaß, A.; Palmieri, P.; Pitzer, R.; Schumann, U.; Stoll, H.; Stone, A. J.; Tarroni, R.; Thorsteinsson, T. *MOLPRO*, Version 2006.1; University College Cardiff Consultants Limited: Wales, U.K.; see <http://www.molpro.net> (accessed Nov 12, 2009).
- (88) Grimme, S. *RICC*; University of Münster: Münster, Germany, 2007.
- (89) Ahlrichs, R.; Furche, F.; Hättig, C.; Klopper, W. M.; Sierka, M.; Weigend, F. *TURBOMOLE*, Version 5.9; TURBOMOLE GmbH: Karlsruhe, Germany; <http://www.turbomole.com> (accessed Nov 12, 2009).
- (90) Ahlrichs, R.; Bär, M.; Häser, M.; Horn, H.; Kölmel, C. *Chem. Phys. Lett.* **1989**, *162*, 165–169.
- (91) Eichkorn, K.; Treutler, O.; Öhm, H.; Häser, M.; Ahlrichs, R. *Chem. Phys. Lett.* **1995**, *240*, 283–289.
- (92) Hättig, C.; Weigend, F. *J. Chem. Phys.* **2000**, *113*, 5154–5161.
- (93) Weigend, F.; Ahlrichs, R. *Phys. Chem. Chem. Phys.* **2005**, *7*, 3297–3305.
- (94) Eichkorn, K.; Weigend, F.; Treutler, O.; Ahlrichs, R. *Theor. Chem. Acc.* **1997**, *97*, 119–124.
- (95) Weigend, F. *Phys. Chem. Chem. Phys.* **2002**, *4*, 4285–4291.
- (96) Weigend, F.; Häser, M.; Patzelt, H.; Ahlrichs, R. *Chem. Phys. Lett.* **1998**, *294*, 143–152.

- (97) NIST Standard Reference Database. <http://webbook.nist.gov/chemistry/> (accessed Nov 12, 2009).
- (98) Davidson, E. R.; Hagstrom, S. A.; Chakravorty, S. J.; Umar, V. M.; Fischer, C. F. *Phys. Rev. A* **1991**, *44*, 7071–7083.
- (99) Colle, R.; Salvetti, O. *Theoret. Chim. Acta* **1975**, *37*, 329–334.
- (100) Miehlisch, B.; Savin, A.; Stoll, H.; Preuss, H. *Chem. Phys. Lett.* **1989**, *157*, 200–206.
- (101) Perdew, J. P. In *Proceedings of the 21st Annual International Symposium on the Electronic Structure of Solids*; Ziesche, P., Eschrig, H., Eds.; Akademie Verlag: Berlin, 1991.
- (102) Levy, M.; Perdew, J. P. *Phys. Rev. B: Condens. Matter* **1993**, *48*, 11638–11645.
- (103) Lieb, E. H.; Oxford, S. *Int. J. Quantum Chem.* **1981**, *19*, 427–439.
- (104) Perdew, J. P.; Kurth, S.; Zupan, A.; Blaha, P. *Phys. Rev. Lett.* **1999**, *82*, 2544–2547.
- (105) Gerenkamp, M.; Grimme, S. *Chem. Phys. Lett.* **2004**, *392*, 229–235.
- (106) Coriani, S.; Marchesan, D.; Gauss, J.; Hättig, C.; Helgaker, T.; Jørgensen, P. *J. Chem. Phys.* **2005**, *123*, 184107.
- (107) Neese, F.; Schwabe, T.; Grimme, S. *J. Chem. Phys.* **2007**, *126*, 124115.
- (108) Hyla-Kryspin, I.; Grimme, S. *Organometallics* **2004**, *23*, 5581–5592.

CT900489G